Abatement of CO$_2$ emissions in Estonian oil shale-based power production

MAI UIBU

TALLINN UNIVERSITY OF TECHNOLOGY
Faculty of Chemical and Materials Technology
Laboratory of Inorganic Materials

Dissertation was accepted for the defence of the degree of Doctor of Philosophy (Chemical and Materials Technology) on October 6, 2008.

Supervisor: Leading Research Scientist Rein Kuusik, Laboratory of Inorganic
                 Materials, Tallinn University of Technology
Co-Supervisor: Professor Andres Trikkel, Tallinn University of Technology

Opponents: Professor Ron Zevenhoven, Åbo Akademi University
                 Professor Rein Munter, Tallinn University of Technology

Defence of the thesis:
                 December 16, 2008, at 11.00
                 Lecture hall: VII-131
                 Tallinn University of Technology, Ehitajate tee 5, Tallinn

Declaration: Hereby I declare that this doctoral thesis, my original investigation and achievement, submitted for the doctoral degree at Tallinn University of Technology has not been submitted for any academic degree.

Mai Uibu

CO$_2$ emissiooni vähendamisvõimalusi Eesti põlevkivienergeetikas

MAI UIBU

TABLE OF CONTENTS

LIST OF PUBLICATIONS

The thesis is based on the following publications:

I   Kuusik R., Türn L., Trikkel A., *Uibu M*. Carbon dioxide binding in the heterogeneous systems formed at combustion of oil shale. 2. Interactions of system components – thermodynamic analysis. *Oil Shale*. **2002**. Vol. 19, No. 2. P. 143–160.

II   Kuusik, R., *Uibu, M.,* Kirsimäe, K. Characterization of oil shale ashes formed at industrial-scale CFBC boilers. *Oil Shale*. **2005**. Vol. 22. No. 4 Special. P. 407–419.

III   *Uibu, M.*, Uus, M., Kuusik, R. CO_2 mineral sequestration by oil shale wastes from Estonian power production. *Journal of Environmental Management*. **2008**. Vol. x. P. 1–8. doi:101016/jenvman.2008.07.012

IV   *Uibu, M.*, Kuusik, R. Mineral trapping of CO_2 via oil shale ash aqueous carbonation: rate controlling mechanism and development of the continuous flow reactor system. *Oil Shale*. **2008**. (In press)

V   *Uibu, M.*, Velts, O., Trikkel, A., Kuusik, R. Reduction of CO_2 emissions by carbonation of alkaline wastewater. Sixteenth International Conference on Modelling, Monitoring and Management of Air Pollution. 22 – 24. Sept. 2008**,** Skiathos, Greece. WIT Transactions on Ecology and the Environment **2008**, Vol. 116, P. 311–320. ISSN 1743-3541. doi:10.2495/AIR08321

In the appendix A, copies of these publications are included.

Closely related publications and international conferences

1)   Kuusik R., Veskimäe H., *Uibu M*. Carbon dioxide binding in the heterogeneous systems formed at combustion of oil shale. 3. Transformations in the system suspension of ash – flue gases. *Oil Shale*. **2002**. Vol. 19, No. 3. P. 277–288.

2)   Kuusik, R., Paat, A., Veskimäe, H., *Uibu, M*. Transformations in Oil Shale Ash at Wet Deposition. *Oil Shale*. **2004**. Vol. 21, No. 1. P. 27–42.

3)   Kuusik, R., *Uibu, M.*, Toom, M., Muulmann, M.-L., Kaljuvee, T., Trikkel, A. Sulphation and carbonation of oil shale CFBC ashes in heterogeneous systems. *Oil Shale*. **2005**. Vol. 22. No. 4 Special. P.421–434 .

4)   Rein Kuusik, Mati Uus, *Mai Uibu*, Gennadi Stroganov, Olev Parts, Andres Trikkel, Valeriy Pepoyan, Aleksander Terentiev, Endel Kalnapenk. Method for neutralization of alkaline waste water with carbon dioxide consisting in flue gas, Patent, EE200600041, priority date: 22.12.2006

5) *Uibu, M.*, Kuusik, R., Veskimäe, H. Abatement of CO_2 emission in Estonian energy sector // VI Intern. Symp. and Exhib. on Environmental Contamination in Central and Eastern Europe and the Commonwealth of Independent States, Prague, Czech Republic, 1 – 4 Sept. 2003. Tallahassee, Florida State University. 2004. 5 p. on CD-ROM.

6) Kuusik, R., *Uibu, M.,* Trikkel, A. CO_2 emission in Estonian oil shale based energy sector - prospects for abatement by wet mineral carbonization // 8th International Conference on Greenhouse Gas Technologies, Trondheim, Norway, 17 – 22 June 2006. Elsevier ltd, 2006. 5 p. on CD-ROM

7) Kuusik, R., *Uibu, M.,* Trikkel, A., Kaljuvee, T., Reuse of waste ashes formed at oil shale based power industry in Estonia. Third Conference on Waste Management and the Environment, 19–23 June 2006, Valetta, Malta. Wessex Institute of Technology Press, 2006. P. 111–120.

8) *Uibu, M.,* Trikkel, A. and Kuusik, R. Transformations in the solid and liquid phase at aqueous carbonization of oil shale ash. Proc. ECOSUD VI 2007, 4–7. Sept. 2007, Coimbra, Portugal. WIT Transactions on Ecology and the Environment 2007. Vol. 106. P. 473-483. ISSN 1743-3541.

9) *Uibu, M.,* Kuusik, R. Concept for CO_2 mineralization by oil shale waste ash in Estonian power production. The 3rd International Green Energy Conference, June 17–21 2007, Vasteras, Sweden. In Proceedings: Paper ID 139, P. 1075–1085.

10) *Uibu, M.*, Kuusik, R. Veskimäe, H. Seasonal binding of atmospheric CO_2 by oil shale ash. *Oil Shale*. **2008**. Vol. 25, No. 2, P. 254–266. doi:10.3176/oil.2008.2.07

Author's own contribution

The contribution by the author to the papers included is as follows:

I   Interpretation of the results, minor contribution

II   Specific surface area measurements, interpretation of the results, major role in writing

III   Planning and conducting the experiments, interpretation of the results, major role in writing

IV   Participating in planning and conducting the experiments, interpretation of the results, major role in writing

V   Planning and conducting the experiments, interpretation of the results, major role in writing

INTRODUCTION

Human activities are generally considered responsible for the so-called greenhouse effect and the consequent climate changes [1]. The concentration of CO_2 in the atmosphere has increased rapidly from 280 ppm since the beginning of industrialization and extensive using of fossil fuels reaching 384 ppm in 2007, an annual growth rate being almost 2 ppm since the year 2000. This increase has been considered being a major factor behind the raise of the earth's temperature. To avoid the risk of global warming and climate change, the anthropogenic CO_2 emissions into the atmosphere should be considerably reduced.

The heat and power production, which is still based mainly on fossil fuels, is a leading contributor to the emission of the greenhouse gas CO_2. Its content in the atmosphere could be stabilized by either increasing the natural/biological binding of CO_2 from the atmosphere or reducing the CO_2 emissions. The latter could be achieved (a) by reducing the fossil energy sources in energy production (e.g. renewable energy, nuclear power, lower C/H ratio), (b) by improving the energy efficiency and energy conversion technologies or (c) by more intensive implementation of the carbon capture and storage (CCS) technologies [1].

In the Republic of Estonia, local low-grade carbonaceous fuel, Estonian oil shale, is used as a primary energy source. Estonian oil shale differs from other fossil fuels in its high proportion of mineral CO_2 in the form of limestone and dolomite, and a higher specific carbon emission factor: 29.1 t C/TJ against 25.8 and 15.2 t C/T in coal and natural gas, respectively. In Estonia, the power sector is the largest CO_2 emitter and is also a producer of huge amounts of waste ash (45–47% of oil shale burnt, dry mass basis).

According to the Kyoto Protocol, during the period of 2008-2013 Estonia is obligated to reduce the emissions of air-polluting greenhouse gases from its territory by 8% as compared to year 1990 level. To reduce the CO_2 emissions several mitigation strategies, projections, legal acts and programs (in particular Estonian National Environmental Strategy, and GHG Emission Reduction Programme for 2003–2012 [2]) have been elaborated and enforced in Estonia. The main options are improving energy efficiency, shift to low-carbon fuels and wider use of renewable energy sources. As the renewable options are currently far from covering Estonia's energy demand, even the use of nuclear power has been under discussion. In order to continue using oil shale as a primary energy source, its environmental impact including CO_2 emission should be diminished.

LIST OF ABBREVIATIONS

AAS	Atomic absorption spectrophotometry
AOD	Argon-oxygen decarburisation
APC	Air pollution control
BD_{CaO}	CaO-binding degree
BD_{CO2}	CO_2-binding degree
BD_{CO2}*	CO_2-binding degree calculated on free CaO basis
BET	Absorption theory by S. Brunauer, P. H. Emmet and E.Teller
CCS	Carbon dioxide capture and storage
CFBC	Circulating fluidized-bed combustion
CO_{2max}	Maximal CO_2-binding capacity
CRW	Carbonated recirculation water
DW	Distilled water
EDX	Energy dispersive X-ray analysis
EDTA	Ethylenediaminetetraacetic acid
FG	Flue gas
GGBS	Ground granulated blast furnace slag
IGCC	Integrated gasification combined cycle
IR	Indissoluble residue in *aqua regia*
k_{CO2}	Decomposition rate of carbonate part of oil shale
k	Mole ratio of $CO_2^{(g)}$ contacted with the pulp and free CaO present in the initial pulp
Ks	Solubility product
LOI	Loss on ignition
MSWI	Municipal solid waste incineration
N_{CO2}	Degree of carbonation
PCC	Precipitating calcium carbonate
PF	Pulverized firing
RW	Recirculation water
SEM	Scanning electron microscopy
SSA	Specific surface area
XRD	X-ray diffraction
α	Conversion rate of dissolved CO_2
ΔG_T	Gibbs energy change (kJ/mol)
ΔH	Reaction enthalpy (kJ/mol)
Ash types: BA	Bottom ash
FA	Filter ash
CA	Cyclone ash
ECO	Economizer ash
ESPA	Electrostatic precipitator ash
INT	Intrex ash
PHA	Air preheater ash
SHA	Superheater ash

1. LITERATURE OVERVIEW

1.1. CO_2 capture and storage

Carbon dioxide (CO_2) capture and storage is a process consisting of the separation of CO_2 from industrial and energy-related sources, transport to a storage location and a long-term isolation from the atmosphere [1].

The capture step involves separating CO_2 from other gaseous products. For the energy sector, there are three main approaches for capturing CO_2 generated from fossil fuel: *post-combustion, pre-combustion* and *oxy-fuel* combustion systems (Fig. 1). *Post-combustion* systems separate CO_2 from a flue gas stream. These systems typically use a liquid amine-based solvent to capture the small fraction of CO_2 (3–15% vol.) present in a flue gas stream, whose main constituent is nitrogen [3]. *Pre-combustion* systems remove CO_2 prior to combustion, including gasification of the primary fuel, water gas shift and CO_2 separation. Although the initial fuel conversion steps are elaborate and costly, the high concentrations of CO_2 produced by the shift reactor (15–60% vol.) and the high pressures are favorable for CO_2 separation. Pre-combustion is most suitable for the power plants that employ integrated gasification combined cycle (IGCC) technology. *Oxy-fuel combustion* systems use oxygen from air-separation unit for combustion of the primary fuel to produce flue gas that mainly consists of water vapour and CO_2. The water vapour is then removed by cooling and compressing [1].
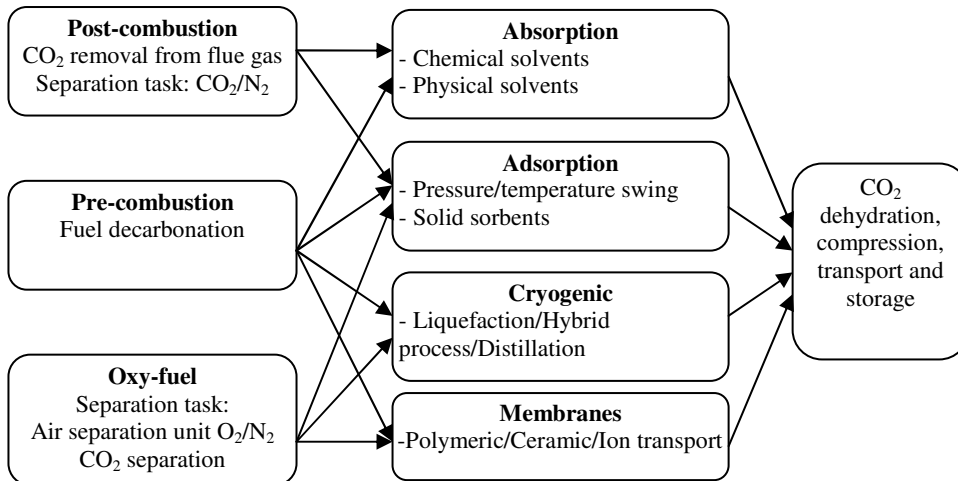

Figure 1. CO_2 capture pathways [4]

However, CO_2-capture systems require significant amounts of energy to operate. This reduces the plant efficiency, because the power plants require more fuel (ca

11–40%) to generate each kilowatt-hour of electricity produced. Net costs of the captured CO_2 for a coal- or gas-fired power plant are 15–75 US\$/tCO_2 [1].

In most cases, after drying and compression the captured CO_2 must be transported to the storage site, since appropriate storage sites are rarely located near the CO_2 source. Transportation by pipelines (under the pressure above 80 bar) is the most common and mature technology. For long-distance transport, CO_2 might also be transported as a liquid by ship (under the 7-bar pressure). The cost of the pipeline transport depends on the flow rate, terrain, offshore/onshore transportation and distance, and is typically 1–8 US\$/tCO_2 for a nominal distance of 250 km [1].

In order for CCS to be a useful option for reducing the CO_2 emission, the captured CO_2 has to be stored isolated from the atmosphere for a long period of time (thousands of years) [1]. The only mature technology currently available is CO_2 storing into geological formations, including oil and gas reservoirs, deep saline formations, and unminable coal beds. In the case of geological storage, the estimated CO_2-storage capacity ranges between 2,000–10,000 Gt CO_2 [1]. Several industrial-scale projects (such as the Sleipner project in the North Sea, the Weyburn project in Canada [5] and In Salah project in Algeria) have been storing CO_2 in geological formations. The estimated cost of the CO_2 storage in saline formations and depleted oil and gas fields is 0.5–8 US\$/tCO_2 injected plus 0.1–0.3 US\$/tCO_2 for monitoring [1].

A potential CO_2-storage option is to inject CO_2 directly into the deep ocean (at the depths greater than 1,000 m, where most of the CO_2 would be isolated from the atmosphere for centuries). Stabilizing the atmospheric CO_2 concentrations between 350 and 1,000 ppm would imply that 2,000–12,000 Gt CO_2 would eventually end up in the ocean on the time scale of thousands of years. The latter figures also represent the upper limit for the capacity of the active CO_2 injection. The cost for CO_2 injection into the ocean at 3,000-m depth has been estimated to be 6–31 US\$/tCO_2. However, little is known about the effect of actively injecting CO_2 on the ocean environment [1]. This option is receiving less and less attention.

Another option for CO_2 storage is the fixation of CO_2 in the form of inorganic carbonates, also known as mineral carbonation or mineral sequestration. Carbonation of alkaline minerals mimics the natural rock weathering and involves the permanent storage of CO_2 as the thermodynamically stable form of calcium and magnesium carbonates [1]. Moreover, magnesium and calcium silicate deposits are sufficiently abundant to fix the CO_2 that could be produced from the combustion of all fossil fuels sources [1, 5]. However, the technology CO_2 sequestration through mineral carbonation has not yet been developed at the full scale due to cost limitations: a power plant equipped with a full CCS system with mineral carbonation would require much more (from 60 to 180%) energy than power plant without CCS. Also, significant environmental impacts of the large-scale mineral carbonation would be a consequence of the required mining (1.6-3.7 tons of silicate rock to store 1 ton of CO_2) and disposal of resulting products that have little or no practical use [1]. It has been estimated that the sequestration costs of current

mineral carbonation (78–310 US\$/tCO$_2$) are high relative to the costs of geological capture and storage options [6].

All in all, even though rules and regulations have been formulated and various technologies suggested, the major break-through in reducing the global CO$_2$ emissions is yet to come.

1.2. CO$_2$ sequestration by mineral carbonation

Mineral carbonation was first mentioned as a concept for CO$_2$ abatement by Seifritz in 1990 [7] and developed by Dunsmore [8] and Lackner [9-12]. Since then, research on the mineral carbonation has divided into several different CO$_2$ binding approaches (Fig. 2) - mainly direct and indirect carbonation [13, 14].

At first, only natural Ca- and Mg-rich minerals such as olivine, serpentine, wollastonite and talc, which are wide-spread and inexpensive, were considered as raw materials [15-18]. Since 1998, the carbonation of industrial wastes such as ashes [19], air pollution control (APC) equipment residues [19, 20] steel slag [21-24] and waste cement [25], which contain considerable amount of Ca or Mg, has also been studied. Although the potential CO$_2$-storage capacity of such waste materials is limited (the amounts of material that may be carbonated are just too small [26]), the possibility of binding CO$_2$ and simultaneously lowering the hazardous effect of waste materials gives this approach an extra value.
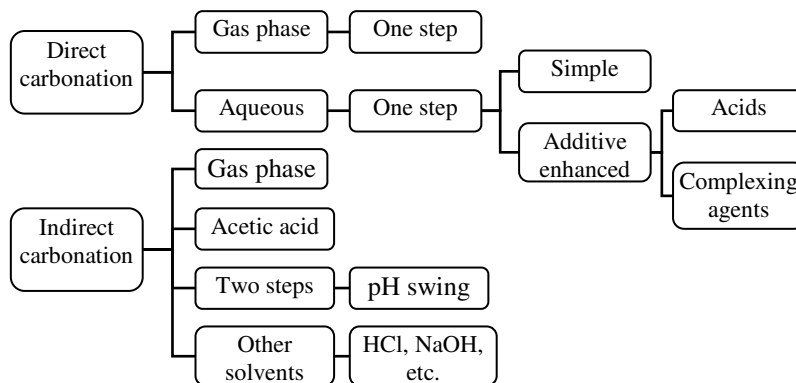
Figure 2.   Main carbonation processes [13, 14]

1.2.1. Direct carbonation of Ca- and Mg-rich minerals and waste residues

Direct carbonation is the simplest approach to the mineral carbonation. The main idea is that the suitable feedstock (natural mineral or solid wastes) is carbonated in one stage. In the case of aqueous process, both the extraction of metals from the feedstock and the subsequent reaction with the dissolved carbon dioxide to form carbonates take place in the same reactor [14].

1.2.1.1. Direct gas–solid reaction

A direct gas–solid reaction of natural minerals, requiring elevated temperatures and pressures (500°C, 340 bar) appears unviable for industrial processes because of very slow reaction rates and thermodynamic limitations [10, 27]. Gas–solid carbonation of MSWI ashes and APC residues gave more promising results [20, 26, 28] in the environment of elevated temperatures (200–500°C) or high pressures (17 bar).

1.2.1.2. Direct aqueous carbonation of natural Ca- and Mg-rich minerals

In the aqueous process, carbonation occurs in the three-phase system (gas–solid–water medium), which considerably increases the reaction rate as compared to gas–solid route.

Direct aqueous carbonation of minerals is a process, in which a slurry of water mixed with pre-treated Mg- or Ca-rich silicates is reacted with carbon dioxide to produce carbonates (Eqs. (1–3)). Carbon dioxide is dissolved in water to form carbonic acid, which dissociates to hydrogen cations and bicarbonate anions. The hydrogen cations react with the mineral, liberating magnesium cations, which, in turn react with bicarbonate to form the solid carbonate [29]. Several silicate minerals achieved carbonation reaction rates sufficient for industrial application at elevated temperatures and pressures [30] and/ore in the presence of additives (Table 1), while being relatively inactive at ambient temperature and under sub-critical CO_2 pressures (below 74 bar).

$$CO_2(g)+H_2O(l) \rightarrow H_2CO_3(aq) \rightarrow H^+(aq)+ HCO_3^-(aq) \qquad (1)$$

$$Ca/Mg\text{-}silicate(s) + 2H^+(aq) \rightarrow (Ca/Mg)^{2+}(aq) + SiO_2(s)+H_2O(l) \qquad (2)$$

$$(Ca/Mg)^{2+}(aq) + HCO_3^-(aq) \rightarrow (Ca/Mg)CO_3(s) + H^+(aq) \qquad (3)$$
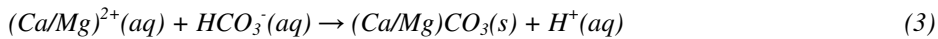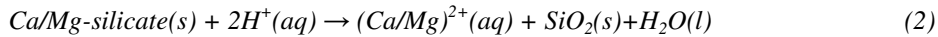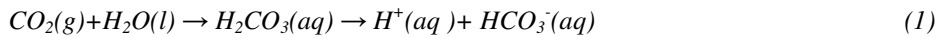
Table 1:   Optimum carbonation conditions and extent of carbonation

Mineral or residue	T, °C	P_{CO2}, atm	Carrier solution	Duration	Extent of carbonation	Ref.
Olivine	185	150	0.64M NaHCO₃, 1M NaCl	1 h	49.5%	[31]
Serpentine	155	115	0.64M NaHCO₃, 1M NaCl	1 h.	75.5%	[31]
Wollastonite	100	40	Distilled water	1 h	81.8%	[31]
Wollastonite	200	20	Distilled water	15 min	70%	[32]
Steel slag	100	19	Distilled water	30 min	74%	[23]

To speed up the kinetics of the direct aqueous carbonation process, various physical and chemical pre-treatment methods [33], as well as mechanical procedures [34] and heat-activation of the minerals [35] with the purpose to enlarge the reaction surface have been studied. Intensified mixing that causes high-energy particle–particle interactions can be used to remove the rate-limiting SiO_2 and carbonate layers to enhance the reaction rate [17]. Certainly, enhancing the reactivity of minerals requires extra energy or chemical additives and thereby increases the costs.

Acids (HCl, acetic acid and citric acid [11]) and complexing agents, while enhancing the dissolution of minerals, can complicate the carbonation/precipitation

step by lowering the pH too much for carbonate precipitation to occur or by the formation of too strong complexes [13]. To execute both reactions in one step a careful optimization is needed.

1.2.1.3. Direct aqueous carbonation of waste residues

One way of bypassing some of the draw-backs of the accelerated carbonation of primary alkaline earth minerals is to use the alkaline waste residues from thermal processes or from construction and demolition activities as a feedstock. As these materials are often associated with CO_2 point source emissions and tend to be chemically more unstable than geologically derived minerals [22], they require a lower degree of pre-treatment and less energy-intensive operating conditions to enhance carbonation yields [22, 36]. Furthermore, after stabilization by the accelerated carbonation, the leaching behavior of the alkaline waste materials such as municipal solid waste incinerator ashes [26, 37, 38], steel slag [22] and APC incinerator residues [19, 28, 39] is improved, allowing for use in civil engineering applications or for safer final disposal to landfill. Accelerated carbonation can be used to stabilize many of the industrial residue streams produced from coal- and oil shale-fired power plants, including pulverized fly ash (PFA) [40], fluidized bed combustion (FBC) [41] and circulating fluidized-bed combustion (CFBC) ashes [42, 43] (Table 2). Beside the effects of carbonation on the mechanical properties of cement-based materials [44], recently the research has also focused on the accelerated carbonation treatment to promote the stabilization degree and to improve the leaching behavior of the treated material [25].

Table 2:   Composition of some calcium silicate-containing waste residues suitable for accelerated carbonation (weight, %)

Sample	CaO	SiO$_2$	MgO	Al$_2$O$_3$	Fe$_2$O$_3$	Ref.
APC	65.04	20.71	1.03	4.83	2.77	[19]
PFA	3.36	46.96	1.76	23.71	11.33	[19]
GGBS	41.38	34.59	6.84	14.02	1.51	[19]
MSWI BA	22.62	10.32	1.61	5.30	0.95	[19]
MSWI FA	35.89	15.29	1.29	6.25	1.11	[19]
Deinking ash	37.69	33.76	3.72	20.12	0.03	[19]
Oil Shale ash	51.53	21.44	7.06	6.76	6.64	[45]
Stainless steel slag	46.66	27.92	9.75	2.91	1.22	[19]
Blast furnace slag	40.60	34.10	10.70	9.40	0.90	[24]
Steel converter slag	43.60	13.90	1.44	1.77	24.10	[24]
Electric arc furnace slag	40.80	26.60	5.83	1.21	0.21	[24]
AOD process slag	60.70	27.60	5.83	1.21	0.21	[24]
Wollastonite	44.50	52.20	0.54	1.48	0.30	[24]

The accelerated carbonation of alkaline solid waste has been up to now primarily investigated through the direct aqueous route [6, 22, 37, 46]. The carbonation of residues does not generally require the extraction of alkaline metals from the solid matrix, since the main reactive species are Ca-containing silicates, oxides and

hydroxides. These minerals behave differently from those containing Mg, as hydration, solvation and carbonation occur under the same operation conditions in a one-stage operation [19].

Accelerated carbonation of steel slag

The accelerated carbonation of waste materials of low solubility in which Ca is generally bound as silicate (steel slag) is in most cases carried out in a water slurry phase (L/S>1 w/w) [21, 22, 47]. Depending on residue composition, different operational parameters have been identified [23, 25, 48] and CO_2 uptake in materials with high content of alkaline oxide silicates, such as steel slag, has shown to be influenced by operational parameters (pressure, temperature, particle size distribution) similarly to carbonation of minerals such as wollastonite; however, optimum operational conditions for the processing of residues were found to be less energy demanding (T = 100°C, p_{CO2} = 19 bar, Table 1). The carbonation reaction was found to occur in two steps; 1) leaching of calcium from steel slag particles into solution; 2) precipitation of calcite on the surface of particles. The first step and, more in particular, the diffusion of calcium through the solid matrix toward the surface appeared to be rate-limiting step. The Ca diffusion was found to be hindered by the formation of a $CaCO_3$ coating and Ca-depleted silicate zone during the carbonation process [23].

Accelerated carbonation of MSWI bottom ash

MSWI BA represents 80% of the incinerator residue produced and is classified as a non-hazardous waste (European Waste Catalogue) consisting mainly of alumosilicate phases and certain amounts of metallic components (8%), including Cr, Ni, Cu, Zn, Ba, Pb, Cd, As, Ti, Mn and Hg. As Ca and Mg contents are typically not high enough for significant CO_2 sequestration, the application of the accelerated carbonation is therefore applied with the aim to attain a chemically stable structure with improved leaching behavior [19, 46].

The carbonation of BA has been investigated to track the mineralogical changes similar to those resulting from natural weathering and to induce a related reduction in trace metal mobility [37, 38, 49]. Recent studies have also focused on the principal carbonation mechanisms and controlling operating parameters, such as temperature, CO_2 partial pressure, water proportion, residence time, as well as particle size [26, 46].

Table 3 gives a summary of the operating conditions for the accelerated carbonation: the water solid ratio is either low-ranged (0.05–0.6 w/w), or indicates to slurry-phase conditions (5–20 w/w); the pressure varies from atmospheric to 17 bar, the temperature is between ambient and 50°C, the CO_2 percentage is 0.03–100% and residence times range from hours to weeks.

Due to the complex chemistry and mineralogy of the material, the mechanisms involved in the carbonation of BA are not yet well known. However, it is likely that more than one alkaline oxide-containing mineral (including Ca and Mg silicates) reacts with CO_2 in addition to calcium hydroxide. Most of the studies reported have considered a simplified carbonation of $Ca(OH)_2$ via an aqueous route

[26, 50]. The rate-limiting steps of the carbonation reaction involve the dissolution of calcium from the solid matrix into the liquid phase and the diffusion of CO_2 into the pores. The kinetics of CO_2 uptake is generally characterized by two reaction steps: (1) an increase in the rate of CO_2 uptake with time, which is followed by (2) a decrease in the rate until an approximately constant value of CO_2 uptake is achieved [26, 37, 46]. The first reaction stage probably involves "faster" reacting minerals such as $Ca(OH)_2$, whereas the second stage may involve other, less reactive, minerals [23]. Therefore, the degree of carbonation should be calculated as the conversion of all Ca-reacting species found in feedstock to calcium carbonate.

Table 3:   Conditions for accelerated carbonation of MSWI BA and APC residues

CO_2 conc.	Pressure	Temperature	Duration	Water proportion	Ref.
Operating conditions for accelerated carbonation of MSWI BA					
10% vol.	Atmospheric	50°C	1 h–4 w	Initial	[50]
20% vol.	Not specified	37°C	2 h-7 d	6.4%	[51]
20% vol.	Atmospheric	Not specified	24 h	Not specified	[52]
100% vol	3 bar	Ambient	0–400 min	0–60%	[46]
0.03% (air)	Atmospheric	Ambient	3–4 d	Slurry phase (L/S 5)	[38]
100%	Atmospheric	Ambient	24 h, 48 h	Not specified	[49]
100% vol.	2–17 bar	Ambient	0–180 min	5–25 % (initial)	[26]
100% vol.	Atmospheric	Ambient	27 d (+49 d)	Initial	[53]
10%, 20%	Not specified	30–50°C	1 h-7 d	2.3–50% (initial)	[37]
0.03% (air)	Atmospheric	40°C	1 h–7d	6% (initial)	[37]
Operating conditions for accelerated carbonation of MSWI APC residues					
0.03% (air)	Atmospheric	Ambient	2-4 w	Not specified	[54]
0.03% (air)	Atmospheric	Ambient	4 w	Not specified	[28]
100% vol.	Atmospheric	200–500°C	6 h	0%	[20]
100% vol.	Atmospheric	300–500°C	0.5–48 h	0%	[28]
0.03;50% vol.	Atmospheric	20–60°C	4–40 d	50% (initial)	[55]
100% vol.	3 bar	Ambient	0–400 min	0–60 %	[46]

Accelerated carbonation of APC residues

APC residues are typically a mixture of the fly ash, carbon and lime; they form as a result of the treatment process to clean the flue gases before they are released to the atmosphere. Due to the high lime content (typically pH>12), and high concentration of heavy metals, soluble salts and chlorinated compounds, APC residues are classified as a hazardous waste. High percentage of readily-active calcium hydroxides makes the carbonation of APC residues potentially suitable for the CO_2 sequestration purposes [20, 28, 46] and also decreases the pH value to the levels corresponding to minimum solubility and regulatory limits (pH<9.5) [25, 55]. Accelerated carbonation induces a mineralogical change in the APC residues: the conversion of hydroxides into carbonates results in a consequent lowering of pH that affects the leachibility of many elements and enhances the acid-neutralization capacity of the material.

The mechanisms governing the APC carbonation are more straightforward than those of BA carbonation, since the reactive species are almost entirely composed of portlandite and CaClOH. In the case of APC residues the kinetics of CO_2 uptake shows the same trend as for BA, although with higher weight gains, which result from higher lime contents, and larger specific surface areas and microporosity [46].

Carbonation affects the leaching at three levels: it causes the decrease of porosity, the lowering of pH and transformation of hydroxides into carbonates. During the carbonation of APC residues via an aqueous route, the following parameters are of critical importance: water proportion (optimal value 0.2–0.3 w/w), particle size (optimal value 212 μm), temperature and CO_2 partial pressure. The CO_2-uptake potential of APC residues reaches 120 g CO_2 per kg APC residues [20, 55].

1.2.2. Indirect carbonation of Ca- and Mg-rich minerals and waste residues

In the case of indirect carbonation the reactive component (Ca or Mg) is first extracted from the feedstock (as oxide or hydroxide) in one step and then reacted with carbon dioxide to form carbonates as the next step.

1.2.2.1. Indirect gas–solid carbonation
The direct gas–solid carbonation of calcium/magnesium oxides/hydroxides proceeds much faster than the gas–solid carbonation of calcium/magnesium silicates [10]. On the other hand, magnesium/calcium oxides are rare in nature and have to be produced from calcium/magnesium silicates. As the carbonation of MgO is significantly slower than the carbonation of $Mg(OH)_2$ [56, 57], the direct gas–solid carbonation process should be divided into several steps: for example, the step of the extraction of magnesium oxide under atmospheric pressure followed by the steps of hydration and carbonation at elevated temperature ($>500^{o}C$) and pressure (>20 bar) [56].

1.2.2.2. Indirect aqueous carbonation of natural Ca- and Mg-rich minerals
The addition of acids and complexing agents in a single-step aqueous carbonation process causes a need for balancing the process conditions between an optimum for the dissolution and for the precipitation step. Therefore, it might be advantageous to perform the aqueous route in two steps [34] in a so-called pH-swing process. The pH-swing process first step, which takes place at low pH, is to dissolve the Mg from serpentine (at $70^{o}C$, under the ambient pressure, using aqueous solution of 1% vol. orthophosphatic acid, 0.9% wt. oxalic acid and 0.1 % wt. EDTA [34]) and the second step, which proceeds at higher pH (pH~9.5 by adding NH_4OH), is to form carbonates. Precipitated solid SiO_2 and iron oxide were removed by filtration before carbonation step. The conditions required to obtain a significant conversion (42–65%) are much milder compared to typical direct aqueous carbonation ($185^{o}C$ and 150 atm). A similar process for leaching Ca and Mg from silicate minerals using sulphuric acid has also been proposed [33] for subsequent carbonation.

Another aqueous carbonation route uses acetic acid for the extraction of Ca^{2+}-ions from a calcium rich feedstock [58]. After separation of the solid SiO_2, the gaseous CO_2 is led into the solution to form $CaCO_3$. The best conversion achieved for wollastonite was about 20% in 60 min under total pressure of 30 bar.

To remove the passivating SiO_2-rim, several in-situ physical activation methods such as intensive stirring [59], internal grinding by glass beads [34] and ultrasonic and acoustic treatment [60] have been studied.

Although numerous mineral carbonation routes consisting of multiple steps and using various additives (CH_3COOH [58], H_2SO_4 [33], HCl [10], NaOH [61]) have been suggested over the last decade, the drawbacks related to the recycling of the acid and other chemicals make the processes too expensive for industrial applications [62, 63].

1.2.2.3. Indirect aqueous carbonation of alkaline waste residues

The processes described in the last chapter could also be applied to carbonating industrial residues that are more easily carbonated [47]. Also, the expensive CO_2 sequestration by indirect carbonation might become economically feasible due to upgrading waste products into products of high commercial value, such as high-purity precipitated calcium carbonate (PCC) or magnesium carbonate [24, 47, 62, 64, 65].

The feasibility of producing $CaCO_3$ from waste cement [64], paper bottom ash [66] and steel slag [66] has been studied. The process is as follows: extracting Ca from waste material using high CO_2 pressures as a first step, followed by precipitation of calcium carbonate from the extracted solution at lower CO_2 pressures as a second step [64]. Production of $CaCO_3$ using this process would cost 136 US$/t $CaCO_3$ for desulphurization purposes and 322 US$/t for obtaining a high-purity $CaCO_3$.

1.3. Basics of aqueous carbonation of lime-based systems

Industrial wastes such as APC residues and ashes from solid fuel combustion often contain a considerable proportion of free lime (20–30%) as the main CO_2-binding compound. Therefore, the mechanism and factors influencing the processes of slaking, dissolution and carbonation of lime are also discussed here.

Industrial powdered calcite is usually produced by bubbling CO_2 through an aqueous slurry of slaked lime (Eq. (4)). The industrial process involves the following steps: (1) calcination of limestone (natural $CaCO_3$ rocks) to produce quicklime (CaO) and CO_2; (2) a slaking process, in which the quicklime is transformed into slaked lime slurry by addition of H_2O; and finally (3) the $CaCO_3$ precipitation reaction, in which the by-product CO_2 mixed with air is bubbled through the $Ca(OH)_2$ suspension [67, 68]. $CaCO_3$ precipitation involves four steps: dissolution of $Ca(OH)_2$, CO_2 absorption into the lime solution, chemical reaction and crystal growth [68].

$$Ca(OH)_2 + CO_2 \leftrightarrow CaCO_3 + H_2O \qquad\qquad (4)$$

1.3.1. Factors affecting lime slaking and dissolution of Ca(OH)$_2$

The reaction of lime and water (e. g. lime slaking) is strongly exothermic. When exposed to water, regardless of its form (liquid, steam, vapor or ice), quicklime exhibits a strong affinity for moisture and adsorbs it into pores. As the water penetrates into the surface pores, heat of hydration is being released. This in turn exerts great internal expansive forces in the lime particle and causes it to fracture, shatter, and then disintegrate into microparticles, in the form of either a crystalline dust or a colloidal suspension, depending on the proportion of water [69].

The slaking reaction can be considered to proceed in three steps: step 1, the conversion of calcium oxide to calcium hydroxide (Eq. (5)) is followed by step 2, the dissolution of calcium hydroxide to give calcium ions and hydroxide ions on the surface (Eq. (6)) and next by step 3, the diffusion of the calcium ions and hydroxide ions into the bulk of the solution (Eq. (7)) [67, 68]. The rate of hydration is influenced by the porosity, the amount of impurities (for example MgO retards reaction rate, while slag forming from silica, alumina or iron clogs the pores), the calcium oxide particle size, the time and temperature of limestone calcination, the amount of water added and agitation [69, 70]. As a function of the stirring efficiency Ca(OH)$_2$ dissolution can be either chemically or diffusion controlled: under moderate agitation (<300 rpm) the overall rate is controlled by diffusion of Ca^{2+} and OH$^-$ ions from the reacting surface, and under more vigorous agitation (>300 rpm) the dissolution of Ca(OH)$_2$ at the surface controls the rate [67, 70, 71].

$$CaO + H_2O \leftrightarrow Ca(OH)_2; \Delta H^o = -65.2 \ kJ/mol \ [70] \tag{5}$$

$$Ca(OH)_2 \leftrightarrow Ca^{2+} + 2OH^- \ (solid \ surface) \tag{6}$$

$$Ca^{2+} + 2OH^- \ (surface) \leftrightarrow Ca^{2+} + 2OH^- \ (bulk \ solution) \tag{7}$$
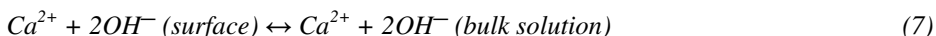
As even minute amounts of extraneous substances present in water affect the extent and rate of lime solubility in water, the water quality can be critically important in lime slaking [69, 70, 72, 73]. In the presence of Ca^{2+}- and OH$^-$-ions the slaking rate drops because the reaction is also controlled by the diffusion of calcium hydroxide away from the surface [70]. Carbonate ions and sulfate ions in the slaking water can form insoluble layers of both CaCO$_3$ and CaSO$_4$, which partially or completely coat the surface and thereby prevent the further dissolution or slow it down [73]. The recycled wastewaters, such as SO$_2$ scrubbing water that contains over 500 mg/l of sulfite, sulfate and bisulfate ions, retard the slaking rate by vitiating the lime reactivity, reducing the hydrate yield and creating coarse to granular particles that sediment rapidly [69]. However, wastewaters from SO$_2$ scrubbing can be employed to dilute a the slaked lime slurry without deleterious consequences [69].

When calcium oxide is immersed in a carbonate-containing aqueous solution, two reactions take place: the usual lime-slaking reaction and the formation of calcium carbonate on the lime surface. The effect of CaCO$_3$ layer on CaO is to hinder both the lime slaking reaction and the formation of further calcium carbonate. At carbonate concentrations 0.01–0.05 M calcium carbonate forms a coherent film on the calcium hydroxide, thus denying water access to surface and

preventing the further dissolution of the slaked lime. At higher carbonate concentrations (>0.05M) the slaking rate starts increasing again due to the direct carbonate attack to the lime surface. This leads to formation of a heterogeneous calcium carbonate/calcium hydroxide surface layer, which is relatively permeable to diffusing species [72].

1.3.2. CO_2 absorption into the lime solution

Carbon dioxide is slightly soluble in pure water, depending strongly on the temperature and partial pressure. At pressures up to 5 atm, the solubility follows Henry's law $[CO_2^{aq}] = K_H * p_{CO2} = 3.65 \cdot 10^{-2} * p_{CO2}$ [74]. CO_2 absorption into the lime solution is favored by both presence of solid particles of $Ca(OH)_2$ and the chemical reaction (Eq. (4)). After CO_2 is absorbed to water it hydrates to form $CO_2(aq)$ or carbonic acid (H_2CO_3) (Eq. (8)) for the most part [68]. Dissolution of CO_2 in water depends on the pH, because the formed H_2CO_3 (CO_2*H_2O) dissociates to HCO_3^- (Eq. (9)) and CO_3^{2-} (Eq. (10)) and, accordingly, the overall concentration of dissolved carbon increases together with the amount of HCO_3^- and CO_3^{2-}-ions formed. The fractional amounts of carbonate species present in solution depending on its pH are presented in Fig 3.

$$CO_2 \rightarrow CO_2 \ (aq) \ (or \ H_2CO_3) \tag{8}$$

$$CO_2(aq) + OH^- \leftrightarrow HCO_3^- \tag{9}$$

$$HCO_3^- + OH^- \leftrightarrow CO_3^{2-} + H_2O \tag{10}$$
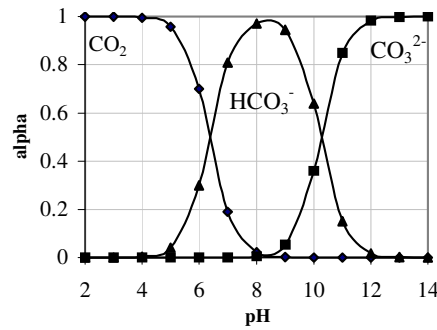
Figure 3.   Dependence of the fractional amounts of all carbonate species α as a function of the solution pH [75]

1.3.3. Chemical reaction of calcite precipitation and crystal growth

Calcite precipitation in the system $Ca(OH)_2$–H_2O–CO_2 starts with the dissolution of $Ca(OH)_2$ and CO_2 that increases the concentration of charged dissolved species (ions) such as Ca^{2+}, OH^-, HCO_3^-, CO_3^{2-}, $CaOH^+$, $CaHCO_3^+$ and uncharged $CaCO_3^0$ [67]. $CaCO_3$ precipitation leads to a decrease in these concentrations. In the initial ascending zone, the dissolution rates of $Ca(OH)_2$ and CO_2 are higher than the

precipitation rate of $CaCO_3$. Maintaining the flow rate of CO_2-containing gas constant, this process leads to the accumulation of an excess of the dissolved $Ca(OH)_2$ in the growth medium [67].

The driving force for $CaCO_3$ precipitation is the supersaturation determined by the product of the ionic concentration of calcium and carbonate ions [68]. Along the batch carbonation process, monitoring of the electrical conductivity and/or pH is normally used as a tool to detect the end point of the reaction. The process of calcium carbonate precipitation by carbonation of slaked lime is a heterogeneous reaction maintained at nearly constant supersaturation. This is reflected generally in the constancy of the values of pH and Ca^{2+} concentration recorded against the time. After $Ca(OH)_2$ consumption, the supersaturation decreases until zero, indicating the end point of neutralization [76].

The reaction of calcite precipitation at high reactant concentration proceeds through the initial precipitation of a kinetically favored amorphous (am) hydrated form (Eq. (11)) [68].

$$Ca^{2+}(aq) + CO_3^{2-}(aq) \leftrightarrow CaCO_3(am)\ (CaCO_3(am)\ Ks=10^{-6}) \qquad (11)$$

Amorphous $CaCO_3$ has been described as consisting of little spherical shapes, whose diameter is less than 1 µm. Because of the higher solubility of the amorphous phase compared to the crystalline phase, the precursor tends to change into the more stable crystalline modification. Transformation from the amorphous to calcite requi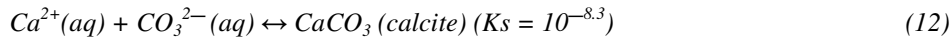res a passage in solution (Eq. (12)). At high CO_2 pressures, the crystallization of amorphous $CaCO_3$ can partially cover the $Ca(OH)_2$ particles inhibiting its dissolution and becoming the primary limitation in increasing the rate of carbonation reaction [68].

$$Ca^{2+}(aq) + CO_3^{2-}(aq) \leftrightarrow CaCO_3\ (calcite)\ (Ks = 10^{-8.3}) \qquad (12)$$

Several factors including pH, supersaturation, temperature, type and concentration of impurities/additives play an important role in the crystal growth and aggregation phenomena. They affect the growth rates of different crystal faces and the surface electrical properties of calcite during its growth in aqueous suspensions [76].

1.4. Estonian oil shale based energy sector as major contributor of CO_2 emissions and waste ash

1.4.1. Greenhouse gas emissions in Estonia

The most significant greenhouse gas (GHG) in Estonia is carbon dioxide. It contributes 87.1% to the total national GHG emissions in CO_2 equivalent and is followed by methane, 9.1%, and nitrous oxide, 3.7% (based on the year 2005 data, [77]). In 2005, the total of GHGs emitted, measured in CO_2-equivalents, was 12,562.3 Gg. Mainly due to the re-structuring and reduction of the industrial production, by 2005 Estonia has reduced its GHG emissions by 52.6 % compared to 1990. Nevertheless, the Republic of Estonia is among the 16 largest emitters of

CO_2 *per capita* in the world (14.1 tons of CO_2 *per capita*). Energy-related activities are the major contributors to GHG emissions (Table 4): a total of 18,381 Gg of CO_2 equivalent was emitted from the energy sector in 2005 (Table 5). That is 89% of the total GHG emissions for that year [77].

The Republic of Estonia signed the Framework Convention on Climate Change at the United Nations Conference on Environment and Development held in Rio de Janeiro in June 1992. In 1994, Estonia ratified the UN FCCC and in 2002 the Kyoto Protocol. Under the Protocol, Estonia is obligated to reduce the emissions of air-polluting GHGs from its territory by 8% as compared with 1990 level during the period of 2008–2012 [77]. Several mitigation strategies, projections, legal acts and programs (including Estonian National Environmental Strategy and GHG Emission Reduction Programme for 2003–2012) have been elaborated and enforced in Estonia. The main goal is to improve the energy efficiency in both the energy sector and the industry, but also for demand side developments.

Table 4:   GHG emissions in Estonia in 1990-2005 [77].

Sources/Sinks	CO_2 equivalent (Gg)			
	1990	2000	2002	2005
Energy	38,834.33	17,180.55	17,293.64	18,381.51
Industrial processes	945.59	587.80	423.35	559.19
Agriculture	3124.40	1,172.20	1,090.92	1,187.00
Land use and forestry	-9,362.90	-8,799.53	-7488.28	-8,096.26
Waste	690.08	797.02	546.44	530.58
Total net emissions	34,231.5	10,938.04	11,866.07	12,562.02

A significant effect on the reduction of CO_2 emission has been achieved due to the introduction of an up-to-date combustion technology, the fluidized-bed combustion of oil shale, at the SC Narva Power Plant. Increasing the fractional amount of the natural gas in the primary energy consumption would decrease the CO_2 emissions because the natural gas is the least carbon-intensive fossil fuel. An important option for reducing the CO_2 emissions is a wider use of renewable energy sources. In Estonia, a biomass is the most essential renewable option, while the wind energy has a smaller importance and the small-scale hydropower minor significance [78].

Table 5:   Emissions from fuel combustion in Estonia in 1990–2005 (Gg CO_2 eqv) [77].

	1990	2000	2002	2005
Energy	38,834	17,180	17,293	18,381
Fuel combustion total	37,630	16,520	16,690	17,600
CO_2 Energy industries	30,770	13,910	13,590	14,340
CO_2 Manufacturing industries	1,790	480	420	1,790
CO_2 Transport	3,020	1,600	1,990	3,020
CO_2 Other sectors	1,950	390	560	1,950
CH_4	90	110	110	90
N_2O	50	40	40	50

1.4.2. Waste flows from Estonian oil shale-based energy sector

Most of the Estonia's energy demand is satisfied by an oil shale; and approximately 67% of the CO_2 emissions come from its combustion. As a fuel, Estonian oil shale is characterized by a high ash content (45–50%), a moderate content of moisture (11–13%) and sulphur (1.4–1.8%), a low net caloric value (8–9 MJ/kg) and a high content of a volatile matter in the combustible part. The dry matter of Estonian oil shale is considered to consist of the three main parts: an organic part, a sandy-clay part and a carbonate part (Table 6). During the pulverized combustion of oil shale, CO_2 is not only formed as a burning product of organic carbon, but it is also formed as a product of decomposition of the fuel's mineral part (*i.e.* carbonates). This makes the carbon emission factor of oil shale relatively high, being 29.1 tC/TJ. The total quantity of carbon dioxide increases up to 25% in flue gases of oil shale combustion [77].

Historically, energy recovery from the oil shale was based on the pulverized firing (PF), which is characterized by low efficiency and high emissions. Recently, new circulating fluidized bed combustion (CFBC) technology has been installed by SC Narva Power Plant, where two units, each of 215 MW capacity are in operation since the beginning of 2005. Due to a lower rate of decomposition of carbonates present in the mineral matter of oil shale (0.6 in the case of CFBC, at operating temperatures 720–800°C and 0.97 in the case of PF at 1,250–1,400 °C), the reduction of CO_2 emissions per unit of energy reached 13–18%.

Table 6: Chemical composition of Estonian oil shale [79]

Organic part		Sandy-clay part		Carbonate part	
Component	%	Component	%	Component	%
C	77.45	SiO_2	59.2	CaO	53.5
H	9.70	CaO	0.7	MgO	2.0
S	1.76	Al_2O_3	16.3	FeO	0.2
N	0.33	Fe_2O_3	2.8	CO_2	44.3
Cl	0.75	TiO_2	0.7		
O	10.01	MgO	0.4		
		Na_2O	0.8		
		K_2O	6.3		
		FeS_2	12.3		
		SO_3	0.5		
Total	100.00		100.0		100.0

Alongside with CO_2 emissions, Estonian energy sector also produces huge amounts of alkaline waste ash. About 5 million tons of oil-shale ash is transported to the ash fields annually. Oil-shale ash contains considerable amount of free CaO (10–25%, depending on the combustion technology). Contacting free lime with water leads to elevated pH-values (pH~13) and makes the ash landfilling by hydraulic transportation highly problematic. As a result, tens of millions cubic meters of alkaline water saturated with Ca^{2+}-ions are being recycled between the plant and

the sedimentation ponds. Before directing the excess water to nature reservoirs, it should be neutralized so that its pH level would fit the environmental regulations (pH<9).

1.5. Summary of the literature review and aim of the study

The emission of GHGs and safe deposition/utilization of the solid wastes are among the most serious problems caused by the extensive usage of low-grade solid fuels in the world heat and power production. The CO_2 emissions could be decreased by reducing the use of fossil energy sources, improving the energy efficiency and/or by more intensive implementation of carbon capture and storage technologies. CO_2 sequestration by mineral carbonation, considering both natural minerals and alkali wastes as CO_2 sorbents, is a prospective option.

In the Republic of Estonia, the energy sector is predominantly (up to 67%) based on a locally-available low-grade carbonaceous fossil fuel, Estonian oil shale. Because of high share of the minerals present in the oil shale, big quantities of the alkali ash are formed (45–47 % of oil shale burnt, dry mass basis) and deposited in open-air ash fields. Depending on the combustion technology, the ash contains a total of up to 25% free Ca and Mg oxides; and therefore it can be considered a CO_2 binder even under natural weathering conditions. In consequence, the ash in question is rich in free lime as its most active component, and because of that it requires stabilization to assure a safe landfilling. Using CO_2 from flue gases as a neutralizing agent, the emission of CO_2 would be diminished.

The aims of this study were to estimate the CO_2-binding ability of the ash at different stages of its transportation and under different deposition conditions and to create a concept for abatement of the CO_2 emissions in Estonian oil shale-based power production using chemical-technological methods.

First, thermodynamical calculations were performed to evaluate the potential of CO_2 binding by the aqueous suspension of oil-shale ash and the theoretical amount of CO_2 bound by the oil-shale ash of average compositions. After considering the thermodynamical limitations, laboratory experiments were carried out to give thorough characterization of the ashes formed in the industrial-scale PF and CFBC boilers. The purpose was to study these ashes as sorbents for binding CO_2 from flue gases in aqueous mineral carbonation processes and to determine the main parameters of the following processes:

- direct one-step aqueous carbonation of the oil shale ash (the process rate determining mechanism was also elucidated);
- indirect aqueous carbonation of the oil-shale ashes by neutralizing the alkaline ash-transportation waters;
- natural weathering of the oil-shale ashes in open-air deposition conditions.

2. THERMODYNAMIC ANALYSIS OF THE REACTIONS OCCURRING IN THE SYSTEM OF ASH WATER SUSPENSION-FLUE GAS *(PAPER I)*

To elucidate the possibilities for reducing the CO_2 emissions, a thermodynamic analysis of the reactions that occur between the gaseous and solid combustion products formed at oil shale combustion was carried out (*Paper I*). Indeed, the thermodynamic analysis performed by calculating the changes in Gibbs free energy ΔG_T only estimates the probability to obtain certain equilibrium compositions in these systems, but gives no information about the limitations of phase contacting and mixing and about kinetic parameters, in particular the time necessary for reaching an equilibrium and the effect of activation energy. In this section, using the HSC software [80], equilibrium composition of the reaction products were calculated for a set of reactions occurring in the system of ash–water–flue gas.

Table 7: Compositions of the ash and flue gas forming at oil shale combustion

Amounts of the ash components contacted with liquid phase			Composition of the flue gas formed at oil shale combustion (λ =1.2)			
Component	Content		Component	From organic part	From mineral part	Total
	%	mol/m³			mol/kg oil shale	
CaO	23.6	227.5	CO_2	22.59	3.92	26.51
SiO_2	24.0	257.9	H_2O	16.98	-	16.98
Al_2O_3	7.0	37.11	N_2	136.70	5.08	141.78
Fe_2O_3	5.0	16.93	O_2	6.04	0.22	6.26
MgO	2.0	46.94	SO_2	0.19	0.54	0.72
K_2O	2.0	15.64	SO_3	-	0.016	0.016
$CaSO_4$	5.5	21.84	Total			192.2
$CaCO_3$	5.5	29.70				
Miscellaneous	23.83	-				

Equilibrium in the system ash pulp–flue gas
When performing the calculations, typical compositions of the ash and flue gas forming at oil shale combustion were used (Table 7). In the pulp, the solid : liquid mass ratio was 1 : 17.5. The compounds including $Ca(OH)_2$, $CaSiO_3$, $Mg(OH)_2$, SiO_2, CO_2, SO_2, $CaCO_3$, $MgCO_3$, $CaCO_3*MgCO_3$, $CaMg(CO_3)_2$, and characteristic species in solution such as $Ca^{(+2a)}$, $Mg^{(+2a)}$, $Na^{(+a)}$, $K^{(+a)}$, $H_2CO_3^{(a)}$, $HCO_3^{(-a)}$, $CO_3^{(-2a)}$ and $OH^{(-a)}$ take part in the reactions. Calculated amount of the flue gas bubbled through the ash pulp varied from 1 to 200 m^3/m^3. To describe the mole ratio of $CO_2^{(g)}$ contacted with the pulp and free CaO present in the initial pulp, factor k was introduced.

As the amount of $CO_2^{(g)}$ contacting with the ash pulp is less than $CO_2^{(g)}$-binding potential of the pulp (260-280 mol/m^3), the $CO_2^{(g)}$ is bound completely (Table 8).
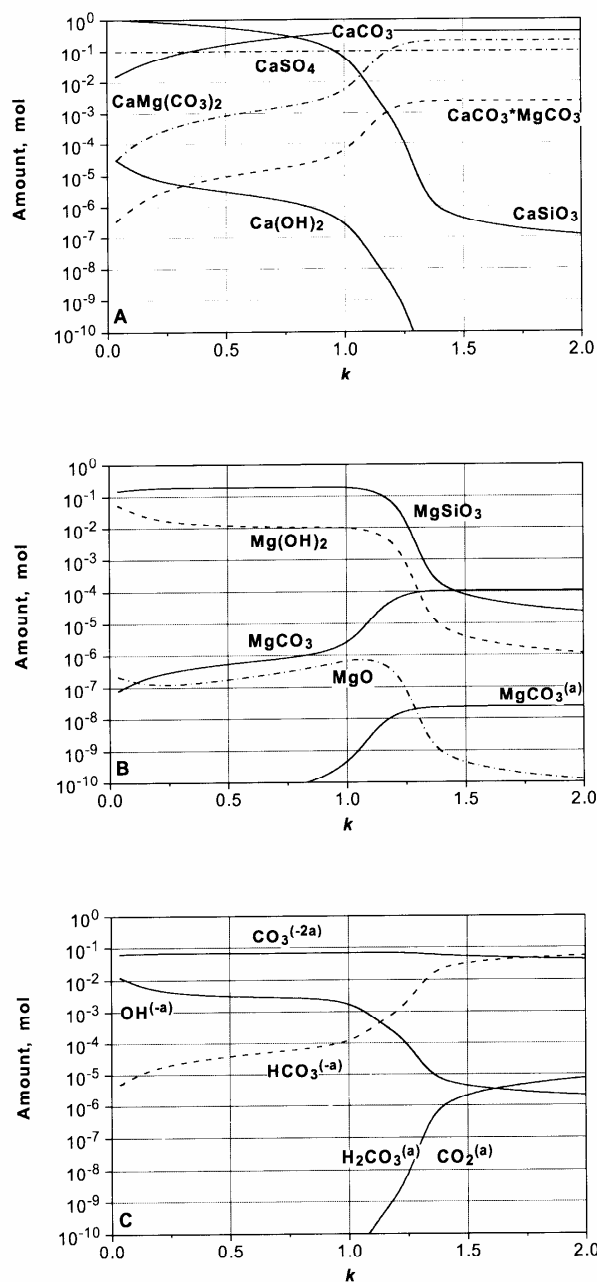
At $k > 1.15$ (about 45 m³ of flue gas per 1 m³ of pulp), the ratio of the $CO_2^{(g)}$ bound to the initial $CO_2^{(g)}$ in the flue gas sharply decreases, and the amount of $CO_2^{(g)}$ bound by 1 m³ pulp stabilizes on the level of $CO_2^{(g)}$-binding potential. The amounts of Ca and Mg hydroxides forming in the reaction of their oxides with water drop quickly when the amount of $CO_2^{(g)}$ increases, whereas the amount of $Ca(OH)_2$ falls more rapidly than that of $Mg(OH)_2$. At first, much Ca is bound into a secondary silicate $CaSiO_3$, but its amount starts to decrease when more $CO_2^{(g)}$ is passed. A possible explanation is the shift of equilibrium of the reaction towards the formation of $CaCO_3$ and SiO_2 at the temperatures below 250 °C (Eq. (13)). $CaSiO_3$ and $Ca(OH)_2$ are preferably used for $CaCO_3$ formation. After most of Ca is used to form $CaCO_3$ and the $CO_2^{(g)}$-binding potential is almost utilized, a formation of a complex carbonate starts and some more $CO_2^{(g)}$ can be bound. Preferably $CaMg(CO_3)_2$ is formed, as the proportional amount of $CaCO_3 \cdot MgCO_3$ is some magnitudes lower (Fig. 4a). While forming complex carbonates almost all available $Mg(OH)_2$ is used up.

Figure 4.   Equilibrium amounts of components (in moles per 1 m³ of ash pulp) depending on factor k: a – Ca compounds; b – Mg compounds; c – $CO_2^{(g)}$ derivatives (*Paper I*).

27

$$CaSiO_3(s) + CO_2(g) \leftrightarrow CaCO_3(s) + SiO_2(s) \qquad (13)$$
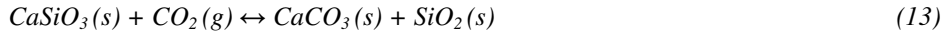
The amounts of dissolved CO_2^-, CO_3^{-2} and HCO_3^- as well as of $KHCO_3$ and $NaHCO_3$ are small, below the $CO_2^{(g)}$ binding potential, but they start to increase at $k > 1.15$. The increase in amount of the flue gas is accompanied by a decrease in the solution alkalinity from $pH \approx 12.7$ to $pH \approx 8.5$. On this pH level the $CO_2^{(g)}$ binding by ash pulp ceases (Fig. 4c). Gaseous sulfur compounds $SO_2^{(g)}$ and $SO_3^{(g)}$ present in flue gas are completely bound, their equilibrium amounts are 10^{-36} or even less. Binding products are $CaSO_4$ and Na_2SO_4, the amounts of other sulfates are negligible.

Table 8: Equilibrium in the system flue gas–ash pulp system depending on the flue gas proportion (*Paper I*).

Component or parameter	Fraction of the flue gas added to 1 m^3 of ash pulp, m^3							
	1	20	30	40	45	50	100	200
	Component amount, moles per 1 m^3 ash pulp							
k	0.03	0.51	0.77	1.02	1.15	1.28	2.56	5.1
$CO_2^{(g)}$ initial	5.82	116	175	233	261	291	582	1164
$SO_2^{(g)}$ initial	0.023	0.468	0.702	0.94	1.053	1.17	2.34	4.68
$CO_2^{(g)}$	10^{-14}	$3 \cdot 10^{-8}$	$2 \cdot 10^{-7}$	$3 \cdot 10^{-6}$	1.57	11.4	286	867
$SO_2^{(g)}$	10^{-36}	10^{-36}	10^{-36}	10^{-36}	10^{-36}	10^{-36}	10^{-36}	10^{-36}
$CO_2^{(g)}$ bound	5.82	116	175	233	260.3	279.6	296	297
CO_2 bound, %	100	100	100	100	99.4	96.1	50.9	25.3
$CO_2^{(a)}$	10^{-14}	10^{-9}	$5 \cdot 10^{-9}$	$3 \cdot 10^{-6}$	0.031	0.200	2.35	3.43
$CO_3^{(-2a)}$	$2 \cdot 10^{-6}$	$4 \cdot 10^{-5}$	$7 \cdot 10^{-5}$	$8 \cdot 10^{-3}$	0.002	0.004	0.003	0.002
$HCO_3^{(-a)}$	10^{-8}	$2 \cdot 10^{-5}$	$6 \cdot 10^{-5}$	$2 \cdot 10^{-4}$	0.72	2.86	8.29	8.81
$H_2CO_3^{(a)}$	10^{-14}	10^{-9}	$5 \cdot 10^{-9}$	$3 \cdot 10^{-6}$	0.031	0.201	2.36	3.45
$Ca(OH)_2$	12.3	10^{-3}	$3 \cdot 10^{-4}$	$4 \cdot 10^{-5}$	$8 \cdot 10^{-11}$	10^{-11}	10^{-12}	10^{-13}
$CaCO_3$	35.5	146	204	263	269	254	248	251
$CaSO_4$	14.6	5.86	6.02	6.18	0.403	0.19	0.247	0.356
$CaSiO_3$	216	127	69	10.2	$2 \cdot 10^{-5}$	$3 \cdot 10^{-6}$	$3 \cdot 10^{-7}$	$2 \cdot 10^{-7}$
$Mg(OH)_2$	46.9	44.6	43.1	41.8	26.5	10.5	1.11	0.71
$MgCO_3$	10^{-12}	$4 \cdot 10^{-8}$	$2 \cdot 10^{-7}$	$2 \cdot 10^{-6}$	0.687	1.87	2.38	2.22
$MgSiO_3$	$4 \cdot 10^{-4}$	2.39	3.84	5.19	3.48	1.40	0.15	0.095
$CaMg(CO_3)_2$	10^{-12}	$3 \cdot 10^{-7}$	$2 \cdot 10^{-6}$	$3 \cdot 10^{-5}$	9.78	25.2	31.2	29.4
$CaCO_3 \cdot MgCO_3$	10^{-14}	$4 \cdot 10^{-9}$	$2 \cdot 10^{-8}$	$3 \cdot 10^{-7}$	0.11	0.29	0.35	0.33
SiO_2	0.014	87	144	201	213	215	217	217
K_2CO_3	10^{-12}	$3 \cdot 10^{-11}$	$4 \cdot 10^{-11}$	$5 \cdot 10^{-11}$	10^{-9}	$2 \cdot 10^{-9}$	$2 \cdot 10^{-9}$	10^{-9}
$KHCO_3$	10^{-10}	$8 \cdot 10^{-8}$	$2 \cdot 10^{-7}$	$7 \cdot 10^{-7}$	0.003	0.02	0.03	0.04
K_2SO_4	0.134	0.29	0.29	0.29	0.396	0.42	0.46	0.50
Na_2CO_3	10^{-10}	$2 \cdot 10^{-9}$	$3 \cdot 10^{-9}$	$3 \cdot 10^{-9}$	$7 \cdot 10^{-8}$	10^{-7}	10^{-7}	10^{-7}
$NaHCO_3$	10^{-10}	$6 \cdot 10^{-8}$	$2 \cdot 10^{-7}$	$6 \cdot 10^{-7}$	0.002	0.007	0.024	0.031
Na_2SO_4	10^{-5}	$3 \cdot 10^{-5}$	$3 \cdot 10^{-5}$	$3 \cdot 10^{-5}$	$4 \cdot 10^{-5}$	$4 \cdot 10^{-5}$	$5 \cdot 10^{-5}$	$7 \cdot 10^{-5}$
Na_2SiO_3	10^{-9}	$3 \cdot 10^{-9}$	$2 \cdot 10^{-9}$	$2 \cdot 10^{-10}$	10^{-14}	10^{-15}	10^{-16}	10^{-16}
pH	12.31	10.66	10.41	9.92	7.74	7.5	6.9	6.8

Diluting or concentrating the ash pulp in the range of 4.4–70 m^3 of water per 1 ton ash causes only slow changes in the equilibrium compositions. Consequently, the fractional amount of the liquid phase is not critical for $CO_2^{(g)}$ and $SO_2^{(g)}$ binding.

Effect of the liquid phase pH on the CO_2 binding
In the case of all the processes where $CO_2^{(g)}$ (from air or flue gas) is in contact with reaction products in the liquid phase, the following general regularities can be drawn:
- The $CO_2^{(g)}$-binding potential depends only on the amount of active components (especially, on the initial amount of Ca and Mg hydroxides) in the liquid phase, but not on the liquid : solid ratio.
- At high pH values (pH = 12–13), $CO_2^{(g)}$ is bound completely, whereas the pH of the solution remains almost unchangeable. $CO_2^{(g)}$ is bound mainly as $CaCO_3$, the formation of other carbonates is of less importance.
- Up to pH = 10–11 the contacted $CO_2^{(g)}$ is bound completely. The pH value of the solution does not characterize the overall $CO_2^{(g)}$-binding capacity of the solution. The main product is $CaCO_3$.
- At pH ≈ 9, a decrease in the ratio of $CO_2^{(g)}$ bound to contacted $CO_2^{(g)}$ can be followed. $CO_2^{(g)}$-binding capacity is utilized to the extent of 90–95 %. Then the formation of $CaMg(CO_3)_2$ as well as of carbonic acid and its ions starts, and it can be followed by the increase in the amounts of $NaHCO_3$ and $KHCO_3$.
- At pH ≈ 8 the ratio of $CO_2^{(g)}$ bound to contacted $CO_2^{(g)}$ drops sharply, and the binding capacity is utilized to the extent of over 98 %. $CaCO_3 \cdot MgCO_3$ appears in the products: however, its role in $CO_2^{(g)}$ binding is of a less importance as compared to the fractional amounts of $CaCO_3$ and $CaMg(CO_3)_2$. The increase in $CO_2^{(g)}$ binding is mainly due to the growth of the amounts of dissolved $CO_2^{(a)}$ and $HCO_3^{(-a)}$.
- At pH ≈ 7.5 the $CO_2^{(g)}$-binding capacity (calculated from the initial content of free CaO and MgO) is completely utilized. Further binding is only due to the slow increase in the amount of dissolved $CO_2^{(a)}$.

If equilibrium is reached, the $CO_2^{(g)}$-binding capacity of the oil shale ash is completely utilized in the system of flue gas–ash pulp (liquid–solid–gas). The main product formed during $CO_2^{(g)}$ binding is $CaCO_3$, the role of other carbonates is of a lesser importance. At pH values 9–10, $CO_2^{(g)}$ binding from the flue gas is complete. A decrease in pH to 8–9 indicates that the $CO_2^{(g)}$-binding potential of the pulp or water is almost utilized. The $CO_2^{(g)}$-binding capacities of ash pulp and of pond water are on the level of 260 moles and 60 or 30 moles (for a working pond or a pond in reserve) of $CO_2^{(g)}$ per 1 m^3 liquid phase, respectively.

The thermodynamical calculations performed show the prospects for CO_2 binding by the aqueous suspension of the oil shale ash and allow evaluating of the favorable pH-region of aqueous suspension and the theoretical amount of CO_2 bound by the oil shale ash of average compositions.

3. EXPERIMENTAL

3.1. Methods for characterization of the ashes

(Papers II, IV: Materials and Methods chapter)

Ash samples were collected from different points within the ash-separation systems of the CFBC and PF boilers at the Estonian Power Plant. The samples were marked as follows:

- for CFBC: bottom ash CFBC/BA, intrex ash CFBC/INT, economizer ash CFBC/ECO, air preheater ash (CFBC/PHA), electrostatic precipitator ashes (taken from the 1st to 4th fields) CFBC/ESPA1-4 and a mixture of the ashes taken from the ash silo CFBC/Mix;
- for PF: bottom ash PF/BA, superheater ash PF/SHA, economizer ash PF/ECO, cyclone ash PF/CA and electrostatic precipitator ashes (taken from the 1st to 3rd fields) PF/ESPA 1-3

All ash samples were analyzed to determine chemical, fractional and phase composition and morphology and specific surface area (Table 9).

Table 9: Methods for characterization of initial materials and reaction products

Properties	Characterization method
Chemical composition[1]	Chemical analysis of the solid phase: total CaO (slightly modified EVS-EN 196-2:1997), free CaO [81], CO_2 (volume method, GOU-1 gas analyzer), total MgO (AAS), total S and its bonding forms (EVS 644:1995), loss on ignition (EVS 669:1996), moisture content (EVS-EN 12048:2000); Chemical analysis of liquid phase: pH, contents of Ca^{2+}, Mg^{2+}, SO_4^{2-} (Spectrodirect spectrophotometer), alkalinity (ISO 9963-1:1994(E)), TDS (HI9032 microprocessor conductivity meter)
Fractional composition[1]	Sieving analysis (EVS-EN 933-1:2000)
Particle size distribution[2]	Beckman Coulter LS 13320 laser diffraction analyzer
Phase composition[3]	Quantitative XRD (Dron-3M diffractometer; diffractograms were analyzed by Siroquant code [82] using full-profile Rietveld analysis [83])
Morphology[4]	SEM (Jeol JSM-8404)
Elemental composition[5]	EDX analysis (HR-SEM Zeiss ULTRA 55; Röntec EDX XFlash 3001 detector)
Specific surface area, pore size distribution	BET and BJH methods (KELVIN 1042 sorptometer, Costech Microanalytical SC)

[1] Performed by H. Ehala and Dr. H. Veskimäe at the Laboratory of Inorganic Materials, TUT
[2] Performed by O. Velts at Lappeenranta University of Technology, Finland
[3] Performed at the Institute of Geology, UT
[4] Performed by Dr. V. Mikli at the Center of Material Research, TUT
[5] Performed by O. Volobujeva at the Department of Materials Science, TUT

3.2. Experimental device for aqueous carbonation of oil shale ash

Batch mode (Papers III, IV: Materials and Methods chapter)
PF ashes, CFBC ashes and model compounds corresponding to oil-shale ash components, such as CaO, $Ca(OH)_2$, MgO, $Mg(OH)_2$, $CaSiO_3$, Ca_2SiO_4, $Ca_3Mg(SiO_4)_2$, $(Ca,Na)_2(Mg,Al)(Si,Al)_3O_7$, $MgSiO_3$ and Mg_2SiO_4, were carbonated in aqueous suspensions in order to evaluate their binding potential as well as the process rate controlling mechanism. Experiment conditions are shown in Table 10. Carbonation of the ash–water suspensions and model compounds was carried out using a model gas whose composition simulated the proportion of CO_2 in flue gases as formed during the oil shale combustion. Carbonation was performed in a glass absorber (diameter 55 mm, water column height 60 or 500 mm) under atmospheric pressure (Fig. 5a).

Table 10:   Methods and conditions of aqueous carbonation of oil shale waste ashes and ash-transportation waters

Materials	Experiment conditions	Characterization of reaction products	Paper
3.2. Transformations and CO_2 binding in the heterogeneous system CO_2–ash–water			
CFBC ashes and PF ashes from EPP	Barboter-type column, batch mode, atmospheric pressure, room temperature, model gas: 10% CO_2 in air	Chemical composition of the solid phase: CO_2, CaO_f, S_{SO4} and the liquid phase: pH, Ca^{2+}, Mg^{2+}, SO_4^2, alkalinity, total dissolved solids (TDS) Elemental composition; Morphology; Specific surface area.	III, IV
Model compounds: CaO, $Ca(OH)_2$, MgO, $Mg(OH)_2$, $CaSiO_3$, Ca_2SiO_4, $Ca_3Mg(SiO_4)_2$, etc	Barboter-type column, batch mode, atmospheric pressure, room temperature, suspension: $(Ca/Mg)/H_2O = 0.0052$; model gas: 10% CO_2 in the air		III
CFBC ashes and PF ashes from EPP and BPP	Barboter-type column, continuous mode; atmospheric pressure, room temperature, model gas: ~15% CO_2 in the air		IV
3.3. CO_2 binding by alkaline ash transportation water			
Ash-transportation waters from EPP	Dispergator-type reactor, atmospheric pressure, room temperature, model gases: FG1 and FG2	Chemical composition of the liquid and solid phases: pH, Ca^{2+}, SO_4^{2-}, alkalinity, TDS, CO_2; Morphology; Particle size distribution.	III, V
Ash-transportation waters from EPP	Barboter-type reactor, batch mode, atmospheric pressure, room temperature, model gases FG1 and FG2.		V
3.4. CO_2 natural binding on ash fields			
CFBC ashes and PF ashes from EPP	Atmospheric pressure, 0.036% CO_2; summer conditions: $+20^o$C (in laboratory), autumn/spring conditions:$+5…+15^o$C and winter conditions:$-22…+3^o$C (in open air)	chemical composition of the solid phase: moisture content, CO_2, CaO_f;	III

Note: EPP = Estonian Power Plant, BPP = Baltic Power Plant

The degree of the carbonation N_{CO2} that indicates how many times the amount of CO_2 entrained into the suspensions exceeds the stoichiometric ratio (C*aO/MgO + CO_2 = CaCO_3/MgCO_3*) varied up to 6. After the carbonation, the suspension was filtered and the solid residue was dehydrated at 105°C. Then both phases were analyzed for chemical composition (Tables 9 and 10). The efficiency of the carbonation process was described by the degree of CO_2-binding BD_{CO2} (*Paper III: Eqs (1) and (2)*). To study the process of deceleration, i.e. the mechanisms that slow down the carbonation process, the samples were also analyzed for specific surface area, surface characteristics and elemental composition.

Continuous mode (Paper V: Materials and Methods chapter)
The continuous-mode aqueous carbonation was optimized by adding reactor-columns (water column height 0.7 m and volume 10 L) working in cascade and setting the pH levels in different reactors in the range of alkaline to almost neutral, prolonging herewith the contact time of the phases (ash, water, CO_2-containing model gas) at optimal conditions for $CaCO_3$ precipitation (Fig. 5b). Ash and water (tap water or circulating process water) were fed to the first reactor-column from which the partly carbonated suspension was led to the next stages for deeper carbonation. The pH of the suspension was controlled by adjusting the flow-rate of incoming CO_2. Samples collected from the bottom side of reactor-columns were filtered and the solid residue dehumidified at 105°C. The liquid and solid phases were analyzed for chemical composition (Tables 9 and 10). The effectiveness of the carbonation process was described by the CO_2-binding degree and the CaO-binding degree (*Paper IV: Eqs. (1–3)*).

3.3. Experimental set-up for CO_2 binding by alkaline wastewater

Dispergator-type phase mixer (Paper V: Materials and Methods chapter)
Neutralization of the alkaline ash transportation water from the ash transportation system of the Estonian Power Plant (Ca^{2+} = 800–1020 mg/l; pH = 13.0–13.1) was carried out in a laboratory dispergator-type batch device (Fig. 5d, Table 10), which provided an effective mechanical mixing of the gas and liquid phases as to increase the interfacial contact surface [84]. The initial ash-transportation water was treated with model gases: FG 1 (15% CO_2 in the air) or FG 2 (15% CO_2 and 0.07% SO_2 in the air). The treated waste-water had pH = 10 after 1 carbonation cycle at CO_2 excess N_{CO2} = 1.5 (the amount of CO_2 passed per the stoichiometric amount according to Eqs (1) and (2) in *Paper V*) and pH = 8 after 3 cycles (N_{CO2}=4.5). The contact time of phases was 1.25-3.75 sec. After separation of the liquid and gas phases the gas was directed into the atmosphere and the liquid phase was either led back into the reactor or sent to filtration, where the solid reaction product was separated and dried at 105°C.

Barboter-type column (Paper V: Materials and Methods chapter)
To compare different technological approaches, also a conventional barboter-type column (Fig. 5c) was used. The experiments lasted until the pH of the treated

wastewater reached pH=10 or 8. The gas phase was analyzed by a TESTO 350 gas analyzer to determine the residual concentration of SO_2. After treatment the suspension was filtered and the solid residue was dehumidified at 105°C.

The liquid and solid phases were analyzed for chemical composition and/or for surface properties and particle size distribution (Tables 9 and 10).
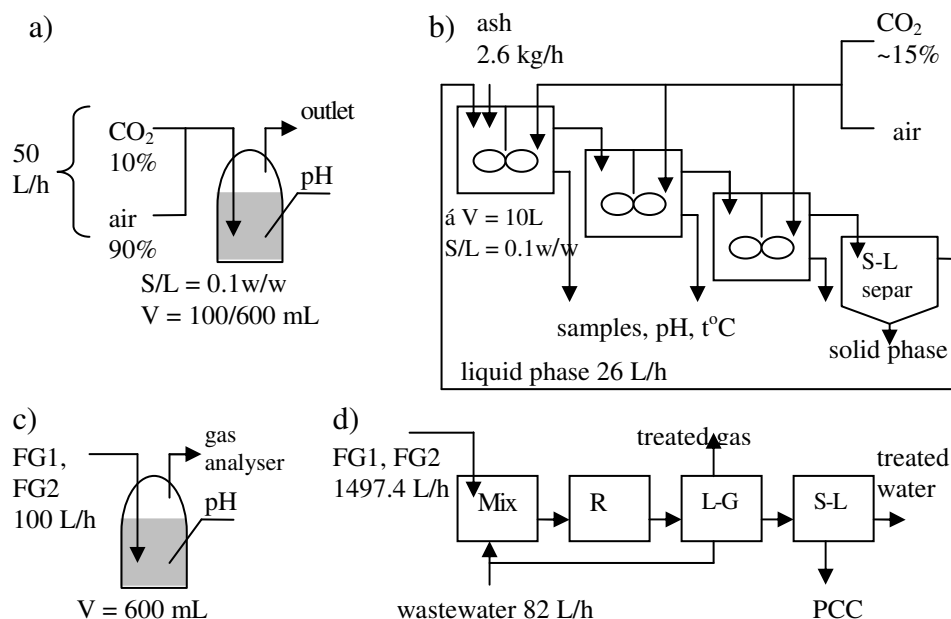

Figure 5. Experimental setups for an aqueous carbonation of the waste ash (a, b) and for an alkaline wastewater carbonation (c, d).

3.4. Experimental setup for a natural CO_2 binding by oil shale ashes

Paper III: Materials and Methods chapter

Model experiments of CO_2 binding in the natural open-air conditions were carried out using CFBC ashes, PF ashes and as a mixture of the two. Initially, the CFBC ash contained 7.10–7.93% CaO_f, the PF ash contained 0.90–1.00% CO_2 and 15.23–20.45% CaO_f and the mixture (50% CFBC ash + 50% PF ash) contained 4.30% CO_2 and 11.17% CaO_f. The ashes were mixed with water (phase ratio 1 : 5 was used to imitate the hydro ash removal and 1 : 0.3–0.9 to imitate the dense slurry technology) and the mixture was loaded into sample holders. These sample bodies were held under summer, autumn/spring and winter temperature conditions (Table 10). After given intervals (1–8 weeks), the sample bodies were taken out of the holders and divided into 6 layers (á 1cm). The layers were dehydrated at 105°C and analyzed for chemical composition (Table 10). The data obtained was used to calculate the amounts of CO_2 and free CaO bound during the experiment (*Paper III: Eq. (3)*) as well as the binding degree (*Paper III*: *Eq. (4)*).

4. RESULTS AND DISCUSSION

4.1. Characterization of oil shale ashes formed in industrial-scale boilers *(Paper II)*

4.1.1. Chemical and phase composition

For the ashes used in the tests, the sharp difference in the operating temperature and fuel particle size [45] results in different behavior of calcium- and sulphur-containing compounds (Table 11 and also *Paper II: Tables 1 and 2*).

Table 11: Characteristics and composition of the oil-shale ashes formed in CFBC and PF boilers

		CFBC ashes			PF ashes		
		BA	INT	ESPA1	BA	CA	ESPA1
Chemical composition, %	CaO_{total}	49.39	47.59	29.52	50.75	49.39	36.08
	CaO_{free}	11.86	18.87	8.45	24.84	22.52	13.56
	MgO_{total}	9.25	13.65	8.33	15.19	14.19	11.39
	S_{total}	4.53	7.76	5.87	1.27	1.33	2.74
	IR	8.85	13.25	42.45	18.21	20.29	26.05
	CO_2	15.14	1.23	4.60	2.75	0.70	1.16
Mineral composition, %	Quartz SiO_2	8.90	5.60	16.80	3.10	3.30	12.0
	Orthoclase $KAlSi_3O_8$	1.30	2.70	12.50	6.60	1.70	3.80
	Albite $NaAlSi_3O_8$	1.60	2.70				
	Illite+Illite-Smectite $Na,K_x(Al,Mg)_2Si_4O_{10}(OH)_2*H_2O,$	2.10	3.10	13.80		6.10	
	Belite Ca_2SiO_4	4.60	7.30	5.30	13.50	15.90	12.30
	Merwinite $Ca_3Mg(SiO_4)_2$	4.70	5.20	3.70	9.40	13.20	6.50
	Tricalcium aluminate $3CaO*Al_2O_3$	1.20	1.40	2.30	2.30	2.20	2.80
	Dolomite $CaM_3(CO_3)_2$	3.90					
	Periclase MgO	4.20	7.00	2.70	7.90	8.70	8.50
	Melilite $(Ca,Na)_2(Mg,Al)(Si,Al)_3O_7,$	1.00	3.60	1.20	17.80	5.80	3.30
	Anhydrite $CaSO_4$	16.20	29.90	9.50	5.40	5.40	16.80
	Lime CaO	11.40	19.90	10.80	26.50	29.30	28.10
	Calcite $CaCO_3$	34.80	4.00	13.50	5.70	2.50	2.00
	Portlandite $Ca(OH)_2$	1.70	2.10			3.10	1.00
	Hematite Fe_2O_3	1.10	2.10	4.30	0.90	1.10	1.60
	Wollastonite $CaSiO_3$	1.40	1.80	3.60	0.90	1.60	0.80
	Σ	100	98.40	100	100	99.90	99.50
	SSA, m^2/g	2.06	2.61	8.00	1.75	0.36	0.61
	k_{CO2}	0.475	0.957	0.841	0.905	0.976	0.960

Due to a considerably higher temperature (up to 1250–1400 °C) when using the PF combustion technology, the rate of the carbonate decomposition is as high as 97–98%, while it is moderate (47–96%) in the case of CFBC technology (boiler temperature 720–800°C). The content of free CaO is higher in the PF ashes (up to 24.84%), while in the case of the CFBC ashes it is relatively high only in the intrex ash (18.87%), but decreases considerably in the electrostatic precipitator ashes (down to 2.82%). In both the CFBC ashes and PF ashes the content of the total CaO decreases and the content of the indissoluble residue increases along the ash separation system.

In the case of the CFBC (Table 11 and *Paper II: Table 1)*, the binding of the gaseous SO_2 occurs in the combustion chamber and the intrex of the boiler. It leads to forming a high sulphur content of the bottom ash (4.53% S) and the intrex ash (7.76% S). The major part of the sulphur is bound to sulphates; only traces of sulphides can be found in the samples taken from the beginning of the ash separation system of the CFBC boilers. In the case of PF, the bound sulphur is more uniformly distributed between the different types of ashes and it is the highest in the precipitator ashes (3.67%, *Paper II: Table 2*).

Quantitative XRD measurements (Table 11 and *Paper II: Tables 5 and 6*) verified the results of the chemical analysis. Compared to the PF ashes, the CFBC ashes contain more calcite and less free lime. Mg was found in both cases mainly as periclase (MgO), and also partially bound to carbonates (dolomite can be found in CFBC bottom ash) or silicates (merwinite, melilite). In the CFBC ashes, the silica compounds are mainly presented by quartz and orthoclase-type K-feldspar, while the PF ashes contain noticeably more secondary silicate – belite and merwinite. A relatively higher content of the secondary silicates can be explained by significantly higher temperatures used in the PF boilers, which leads to the formation of melted phases initiating the reactions between free CaO and quartz or silicates.

4.1.2. Particle size distribution

The particle size of the CFBC ashes varies in a very wide range *(Fig. 6, Paper II: Table 3)*. The bottom ash is the coarsest one (~45% of the particles have a diameter of >0.63 mm), the intrex ash particles are an average size (90% of the particles have a diameter of 0.4–0.045 mm) and the electrostatic precipitator ashes are the finest (85–95% of the particles have a diameter less than 0.045 mm). An article distribution of the PF ashes *(Fig. 6, see also Paper II: Table 4)* is more homogeneous with few particles having a diameter over 0.63 mm.

The above-mentioned dissimilarities in the chemical and fractional compositions of the different ash types observed for various combustion technologies are caused by several circumstances, the particle size composition of the fuel fed to the boiler being the most important of them. For the PF boilers, an average median measure of the fuel fed to the boiler is 35–60 μm, and the rest on sieves with aperture size 90 and 200 μm is 20–40 and 10–25%, respectively. The fractions differ noticeably by their chemical composition [45]. The material fed to the CFBC boilers belongs

predominantly to the size range 1–10 mm. Fine particles of the pulverized oil shale and ashes melt and agglomerate forming larger particles, while in the case of the CFBC, the main part of fine fractions is formed as a result of the intensive attrition of particles in the fluidized bed.
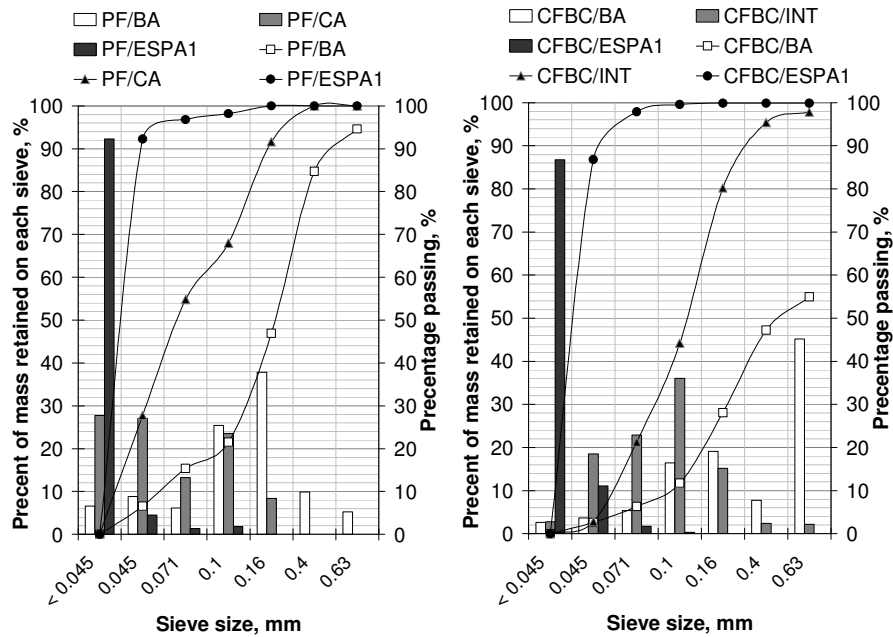

Figure 6. Grain-size composition of PF ashes and CFBC ashes.

4.1.3. Physical structure and surface characteristics

Comparison of SEM photos of the ash samples shows that particles of the CFBC ashes formed at moderate temperatures (750–800°C) are characterized by an irregular shape as well as by a porous and uneven surface (Fig. 7a, *Paper II: Fig. 2*). A glassy phase is not formed.
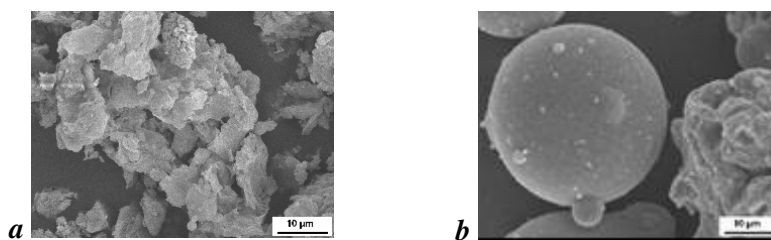

Figure 7. SEM pictures of (a) CFBC/ESPA1 and (b) PF/CA, magnification 2000×.

In the case of PF ashes, the glassy phase significantly affects the formation of the particle shape and surface properties: the particles are characterized by a regular

spherical shape with a smooth surface (Fig. 7b, *Paper II: Fig. 3*). It was shown that along the ash separation system the porous irregular-shaped particles are replaced more and more by regular smooth spherical particles (an electrostatic precipitator ash).

BET measurements (Table 11 and *Paper II: Tables 1 and 2*) showed significant differences in the physical structure of the CFBC ashes and PF ashes: depending on the ash type, the differences in SSA were up to a factor of ten times. While the specific surface area of the CFBC ashes can reach 8.00 m^2/g, the SSA of the PF ashes is within the 0.36–1.75 m^2/g range. This is caused by more intensive sintering of the PF ashes at boiler temperatures. Pore distribution analysis of the ashes showed that the pore volume of the CFBC ashes (CFBC/ESPA1) is contributed by a wide range of pores (Dp>2 nm), while for the PF ashes (PF/CA) the dominating pore diameter is considerably smaller – below 3 nm (Fig. 8). Thereby, the PF ashes are expected to be more extensively influenced by the formation of reaction products on the surface of particles and by pore plugging. This could reduce mass transfer rates.
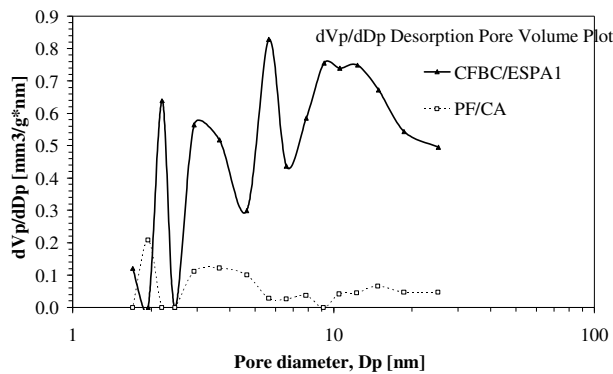

Figure 8.   Pore distribution of the PF ashes and CFBC ashes *(Paper III)*.

Thus, the reactivity of waste ashes towards CO_2 is determined by their chemical and phase composition as well as by the physical structure of the ash particles. Oil shale ashes formed in the boilers operating at different combustion technologies differ significantly in their chemical and phase compositions as well as by surface properties.

4.2. Concept of CO$_2$ mineralization by the oil shale waste ash *(Paper III)*

Based on our investigations relating to the characteristics and reactivity of the oil shale ashes as well as on the literature data, the oil shale ash could be qualified as a sorbent for CO_2 aqueous sequestration. A concept of the CO_2 mineral sequestration by waste oil shale ash has been generalized in Fig. 9, where the proposed technological methods are outlined.

37

The process of ash hydro-separation and depositing is currently in a rather basic state: the ash is hydro-transported into wet open-air deposits, where the solid particles precipitate and the excessive water drains to the lower part of the ash field. After sedimentation the draining water is led back to the beginning of the cycle through a back-flow channel. Together with transportation of the ash particles, other processes including lime slacking, dissociation of forming portlandite and dissolution of different salts also occur. As a result tens of millions cubic meters of alkaline water (pH level 12–13) saturated with Ca^{2+}, K^+, SO_4^{2-} and other ions is recycling between the plant and the sedimentation ponds. In consequence, a certain amount of CO_2 is bound from the air by alkaline transportation water and by the ash during hydraulic transportation and open-air deposition.
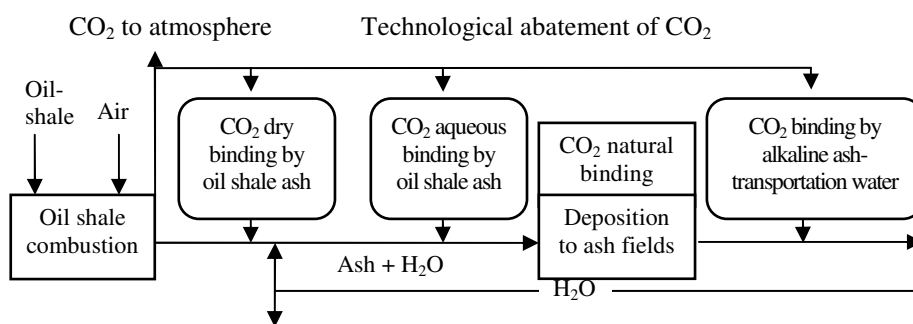

Figure 9. Concept of CO_2 mineral sequestration by a waste oil shale ash (*Paper III*).

According to our initial estimates, the amount of CO_2 emitted during the oil shale-based heat and power production could be diminished by intensification of the natural CO_2-binding processes that occur during ash transportation and deposition. The most extensive effect could be achieved by treating the ash–water suspensions and the ash transportation waters with CO_2-containing flue gases. CO_2 dry binding in the flue gas channel by the oil shale ash [43] has not been a subject of the current investigation.

4.3. Transformations and CO_2 binding in the heterogeneous system CO_2–Ash–Water

Transformations in the heterogeneous system CO_2–oil-shale ash (PF)–water were experimentally first described in one of our earlier papers [40]. Basing on thermodynamic calculations (*Paper I*), the pH of suspension was chosen as a main indicator for describing and directing the carbonation process an in an aqueous media. The binding properties of different types of ashes (*Paper II*) in batch mode, as well as the binding potential of various oil-shale ash components were evaluated and presented in *Paper III*. The behavior of lime as the key component of ash in various conditions was studied and the mechanism of the process deceleration

38

proposed in *Paper IV*. As the next step, a laboratory-scale continuous-flow reactor system for aqueous carbonation of oil-shale ash was worked out and preliminary results were presented in *Paper IV*.

4.3.1. Batch reactor *(Paper III)*

4.3.1.1. Model compounds

The CO_2-binding potential of various oil-shale ash components was evaluated in aqueous carbonation experiments with model compounds including CaO, $Ca(OH)_2$, MgO, $Mg(OH)_2$, $CaSiO_3$, Ca_2SiO_4, $Ca_3Mg(SiO_4)_2$, $(Ca,Na)_2(Mg,Al)(Si,Al)_3O_7$, $MgSiO_3$ and Mg_2SiO_4. The experimental setup and conditions are presented in Chapter 3.2. The duration of the carbonation experiments was 20–40 min, during which 3–5 times the stoichiometric amount of gaseous CO_2 (N_{CO2}) was contacted with the suspension (100 mL).
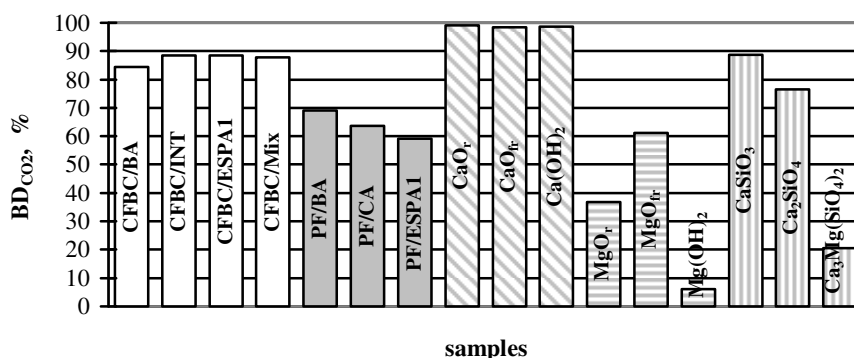

Figure 10. Extent of CO_2-binding at aqueous mineral carbonation of CFBC ash, and PF ashes and model compounds (*Paper III*)

The results of the binding experiments indicated that:
- CaO and $Ca(OH)_2$ were the most active toward CO_2. The BD_{CO2} of these compounds was close to 100% (Fig. 10).
- Ca-silicates also displayed a good CO_2-binding efficiency under the experimental conditions (atmospheric pressure and room temperature): $CaSiO_3$ reached up to 88.7% and Ca_2SiO_4 up to 76.4% of their maximal CO_2-binding potential (Fig. 10). Reactivity of the synthetic/secondary compounds differed significantly from that of the natural minerals, which were treated with CO_2 at 160°C and under 20 bar [15]. Changes that occur with the belite particle as a result of aqueous carbonation are shown in Fig. 11: the Ca-content inside the particle decreases (Fig. 11b) and Ca precipitates on the particle surface as a $CaCO_3$ layer (Fig. 11c).
- MgO showed a moderate CO_2-binding activity: the BD_{CO2} varied from 36.9 to 61.2% (Fig. 10). A freshly-synthesized MgO_{fr} possesses a higher CO_2-binding degree than a commercially purchased MgO_r.

- The CO_2-binding ability of $Ca_3Mg(SiO_4)_2$ was considerably lower (BD_{CO2}=20.6%). We expected that under the experimental conditions melilite and Mg-silicates would not be active toward CO_2. According to the literature data, Mg-silicates are much more stable than Ca-silicates, as the bonds inside the Mg-silicate molecule are difficult to break in these mild conditions [86]. Therefore, in addition to free lime, Ca-silicates $CaSiO_3$ and Ca_2SiO_4, and periclase MgO should also be taken into account while calculating the maximal CO_2-binding potential of oil-shale ashes.
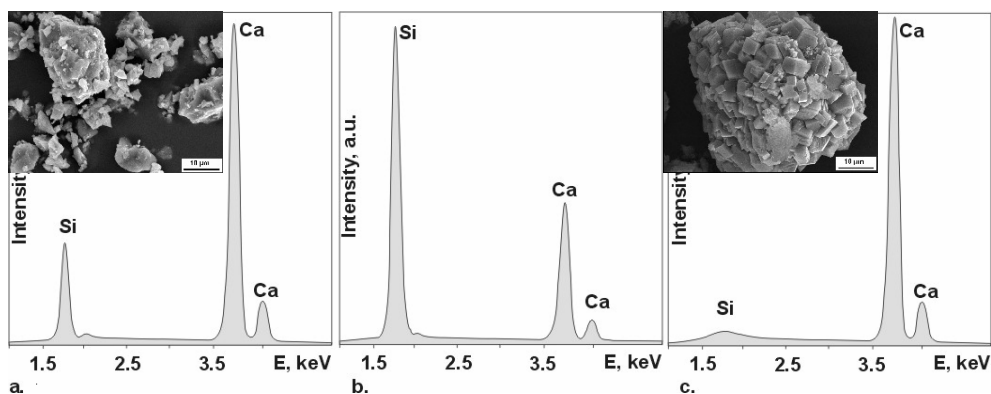

Figure 11. EDX analysis of a belite particle before (a) and after carbonation (b-inside the particle and c- crystals on the particle surface) (presented at GHGT-8 [85])

4.3.1.2. Comparison of CFBC ash and PF ash

The experimental setup and conditions are presented in Chapter 3.2. The duration of the carbonation experiments was 30–90 min, during which 1.2–6 times the stoichiometric amount of gaseous CO_2 (N_{CO2}) was contacted with the ash suspension (600 mL).

Laboratory batch tests demonstrated that oil-shale ashes formed in boilers using different combustion technologies differ noticeably in their reactivity towards CO_2 in aqueous suspensions (Table 12; Fig. 10), as well as in the amount of CO_2 bound.

Compared to the PF ash, it is possible to carbonate the CFBC ash to a greater extent; in most cases it is possible to lower the pH of the aqueous suspensions of its solid residue below pH = 9 (Table 12, with the exception of CFBC/BA – full carbonation is apparently inhibited due to the coarse fractional composition, Fig. 6b). This parameter is important in reference to deposition of carbonated ash. Higher pH values (10.9–11.9) result from a higher free CaO content (0.57–3.47%) in the solid residues of the carbonated PF ashes. Apparently, the lack of porosity in PF ashes limits the availability of a portion of free CaO for reaction with CO_2.

The degree of binding calculated on a free CaO basis (BD_{CO2}*) exceeds 100% for both CFBC ash (140–160%) and PF ash (110–180%. This is explained by the fact that components such as Ca-silicates and MgO present in the oil-shale ash also take part in CO_2-binding reactions. When additional CO_2-binding components like

free MgO, CaSiO$_3$, and Ca$_2$SiO$_4$ are taken into account, BD$_{CO2}$ reached 83–98% for CFBC ash and 48–73% for PF ash. However, due to the lower content of free CaO, the CO$_2$-binding capacity of CFBC ashes in the aqueous carbonation process was lower. The amount of CO$_2$ bound by 1 t of ash depended on the process conditions, reaching ~160 and 100 kg for PF ash and CFBC ash, respectively (Table 12). The total amount of CO$_2$ present in the ash after treatment averaged up to 170 kg/t.

Table 12:   Composition of the carbonized solid phase and some characteristics of the process (*Paper III*)

Ash type	CO$_2$	CaO$_f$	BD*$_{CO2}$[1]	BD$_{CO2}$	pH[2]	CO$_2$ bound, kg/ash, t	
	%					In process	Total
CFBC/BA	23.29	0.88	142.50	84.40	11.60	103.70	232.90
CFBC/INT	15.51	0.43	145.40	88.50	9.60	145.60	155.10
CFBC/ESPA1	12.68	0.18	171.30	88.60	7.20	88.60	126.80
CFBC/MIX	16.09	0.20	158.90	87.80	8.90	104.70	160.90
CFBC/average	17.00	0.50	173.70	86.80	9.00	100.00	170.00
PF/BA	19.46	1.41	104.50	69.00	11.60	167.10	194.60
PF/CA	17.18	0.61	109.90	63.70	10.90	164.80	171.80
PF/ESPA1	12.96	0.75	121.40	59.10	11.00	118.00	129.60
PF/average	17.10	0.90	112.60	64.90	11.00	160.00	171.00

[1] - calculated on free CaO basis
[2] - pH of the aqueous suspension of the solid residue

4.3.2. Process rate-determining mechanism *(Paper IV)*

As shown in the previous chapters, the operating conditions of PF and CFBC boilers significantly affect the composition, physical structure, particle surface properties and, in its turn, chemical reactivity of the forming ashes. In the context of CO$_2$ sequestration and ash stabilization, the availability of lime for hydration and carbonation reactions is of a key importance.

   Low porosity and small-size pores in PF ashes limit the availability of free lime among other components for reaction with CO$_2$, which can easily lead to process deceleration. Therefore, to study process deceleration in the heterogeneous system ash - water - CO$_2$, the PF cyclone ash was chosen as the least porous but also the most typical PF ash (it amounts to 60% of the total PF ash produced). CFBC/Mix12 ash sample was taken to represent the CFBC ashes for comparative experiments. Next, simplified distilled water based batch systems as described above do not correspond to the real continuous-flow processes, where the suspension liquid phase is continuously saturated with different salts leached from the heterogeneous composition of oil-shale ashes. Therefore, distilled water (DW), recirculation water (RW; pH = 13; TDS = 11.4 g/L; Ca^{2+} = 730 mg/L; SO$_4^{2-}$ = 2.8 g/L; OH$^-$ = 64.25 mmol/L) from the ash separation system of the Estonian Power Plant and carbonated recirculation water (CRW; pH = 7.5; TDS = 6.8 g/L; Ca^{2+} =

450 mg/L; SO_4^{2-} = 2.7 g/L; HCO_3^- = 60.75 mmol/L) were used as liquid agents in comparative experiments.
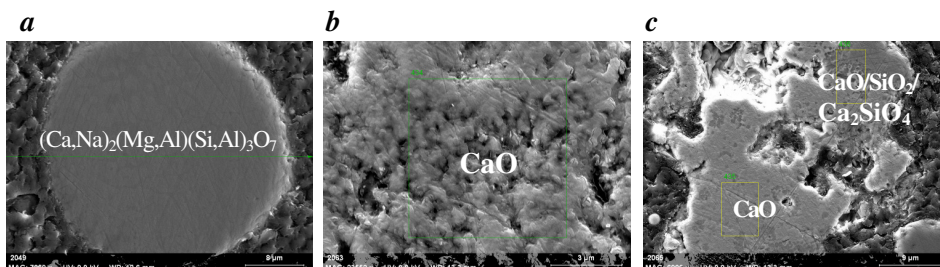

Figure 12. Different types of the particles present in PF cyclone ash (PF07/CA) and their chemical composition (*Paper IV*)
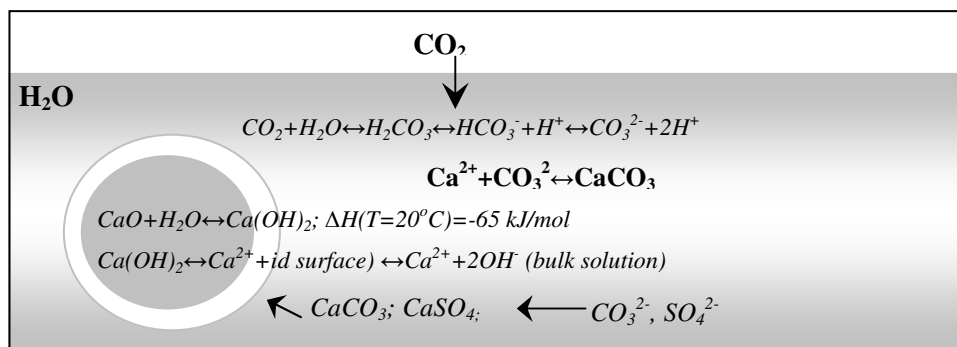

Figure 13. Reactions of lime at CO_2 aqueous sequestration by oil-shale ash (*Paper IV*)

When PF/CA is immersed into DW, slaking of lime-containing particles (Fig. 12b,c) occurs. As the water penetrates into the surface pores, heat of hydration is released and this exerts internal expansive forces in the lime-containing particles (the molar volumes of $Ca(OH)_2$ and CaO are 33.078 and 16.79 mL/mol, respectively [80]). This causes the particles to fracture and disintegrate (Fig. 15a). The conversion of CaO to $Ca(OH)_2$ is followed by the dissolution of $Ca(OH)_2$ to give Ca^{2+}-ions and OH^--ions at the surface of the particles and finally, by the diffusion of Ca^{2+}- and OH^--ions into the bulk of solution (Fig. 13) [68, 70]. The solution becomes deeply alkaline (pH = 12.9) and oversaturated with Ca^{2+}-ions (Ca^{2+} = 1,400–1,500 mg/L, Table 13). The homogeneously melted particles (Fig. 12a) are not affected by hydration (*Paper IV: Fig. 5a*) and are not likely to participate in carbonation reactions during short reaction times (15–45 min) at mild conditions (room temperature, atmospheric pressure, 10% CO_2 in model gas mixture).

As CO_2-containing model gas is bubbled through the ash–water suspension, $CaCO_3$ precipitation reaction takes place (see Fig. 13). During carbonation, the pH

and concentration of Ca^{2+}-ions in the liquid phase stay on a high level until almost all free lime is realized (~2% of unreacted lime in the solid residue, Table 13; Fig. 14a,b). Then the pH of the suspension liquid phase and the concentration of Ca^{2+}-ions decrease rapidly until stabilizing at pH~7.5 and Ca^{2+} = 300 – 400 mg/L (Table 13, Fig. 14a). After carbonation (the solid residue contains 30–36% $CaCO_3$) the ash particles are covered with a porous and permeable product layer (Fig. 15c), as SSA increased to 10–13 m^2/g (see Table 13).

Table 13: Carbonation of the aqueous suspensions of oil-shale ash: composition of the solid and liquid phases (*Paper IV*)

Suspension composition	Composition of the liquid phase						Composition of the solid phase			
	pH	Ca^{2+}	Mg^{2+}	SO_4^{2-}	OH^-	CO_3^{2-}	HCO_3^-	CO_2	CaO_f	SO_4	SSA
		mg/L			mmol/L			%			m^2/g
Initial ashes											
PF07/CA								1.49	23.44	4.56	0.44
PF07/CA* (slowly hydrated by the moisture of air during 8 months)											1.18
PF08/CA								1.13	21.68	3.72	0.47
PF08/CAhydr (hydrated by the added water)											1.48
CFBC07/Mix12								12.29	8.23	6.15	6.32
Ash + distilled water											
PF07/CA	12.9	1500	0	N.a.	56.5	2.0	0.0	1.87	20.8	3.70	1.95
PF08/CA	12.9	1400	0	980	54.0	2.0	0.0	2.24	18.83	2.88	1.62
Ash + recirculation water (pH=13; TDS=11.4g/L;Ca^{2+}=730mg/L, SO_4^{2-}=2.8g/L; OH^-=64.3 mmol/L)											
PF07/CA	13.3	1120	0	N.a.	77.5	4.0	0.0	1.66	21.64	3.93	1.62
PF08/CA	13.3	1060	0	3030	75.5	7.0	0.0	1.71	21.53	3.41	1.10
PF08/CA hydr	13.3	1020	0	3285	66.0	8.0	0.0	1.63	21.65	3.32	2.60
Ash + carbonated recirculation water (pH ~ 7.5; TDS = 6.8g/L; Ca^{2+} = 450mg/L; SO_4^{2-} = 2.7g/l; HCO_3^2 = 60.8mmol/L)											
PF07/CA	12.6	140	0	N.a.	25.0	7.0	0.0	3.1	20.82	4.16	2.21
PF08/CA	12.7	60	0	2805	15.5	15.0	0.0	2.62	22.36	3.62	1.77
PF08/CA hydr	13.3	1020	0	3110	71.5	7.0	0.0	2.96	19.66	3.47	4.01
Ash + distilled water + model gas (10% CO_2, 90% air)											
PF07/CA	7.5	430	18	N.a.	0.5	1.0	0.0	15.98	2.02	2.88	13.7
PF08/CA	7.5	340	36	826	0.0	1.0	1.5	13.61	4.54	2.54	10.2
CFBC07/Mix12	7.5	520	78	N.a.	0.0	0.5	1.0	16.58	1.26	5.67	13.2
Ash + recirculation water (pH=13; TDS=11.4g/L;Ca^{2+}=730mg/L, SO_4^{2-}=2.8g/L; OH^-=64.3 mmol/L)+ model gas (10% CO_2, 90% air)											
PF07/CA	7.5	130	42	N.a.	0.0	5.0	22.5	7.05	17.14	3.84	2.96
PF07/CA*	7.5	310	30	4245	0.0	2.0	2.0	16.92	1.97	2.61	21.2
PF08/CA	7.5	140	24	3055	0.0	6.0	25.0	5.89	18.17	3.34	2.36
PF08/CA hydr	7.5	60	36	3440	0.0	4.0	12.0	11.99	6.97	2.71	5.06
CFBC07/Mix12	7.5	400	24	N.a.	0.0	1.0	3.0	16.99	1.17	6.12	13.0
Ash + carbonated recirculation water (pH~7.5; TDS = 6.8g/L; Ca^{2+} = 450mg/L; SO_4^{2-} = 2.7g/l; HCO_3^{2-} = 60.8mmol/L) + model gas (10% CO_2, 90% air)											
PF07/CA	7.5	180	42	N.a.	0.0	3.0	30.5	4.90	18.47	3.92	2.08

N.a. - not analyzed
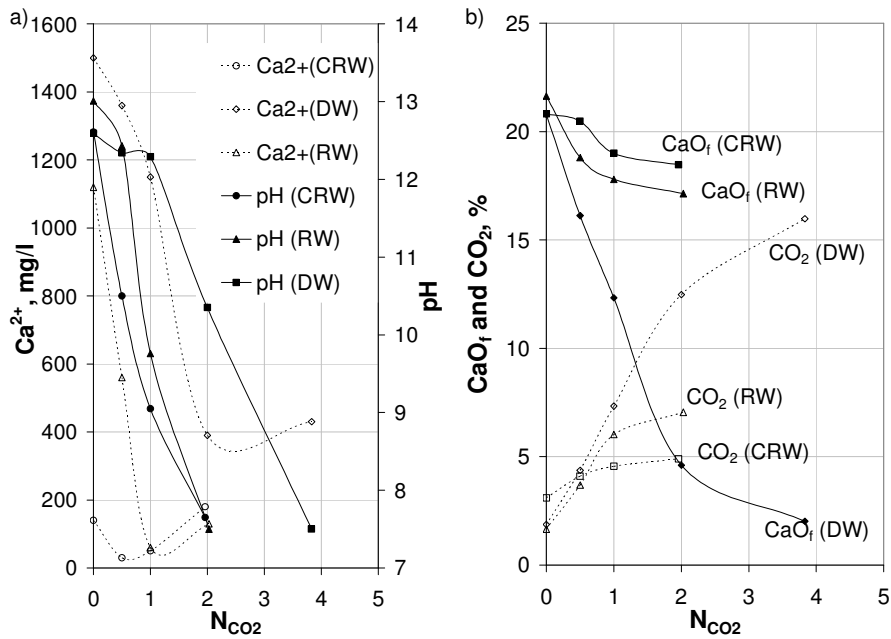
Figure 14. Carbonation of the aqueous suspensions of PF ash (PF07/CA): Dependences of (a) Ca^{2+} content and pH of the liquid phase and (b) CO_2 and free CaO contents in the solid phase on the extent of carbonation (N_{CO_2}) *(Paper IV)*

Figure 15. SEM images of PF ash (PF07/CA) immersed into DW (a) or into CRW (b) and carbonated in the heterogeneous systems of (c) PF07/CA + DW + CO_2 containing model gas or (d) PF07/CA + CRW + CO_2-containing model gas

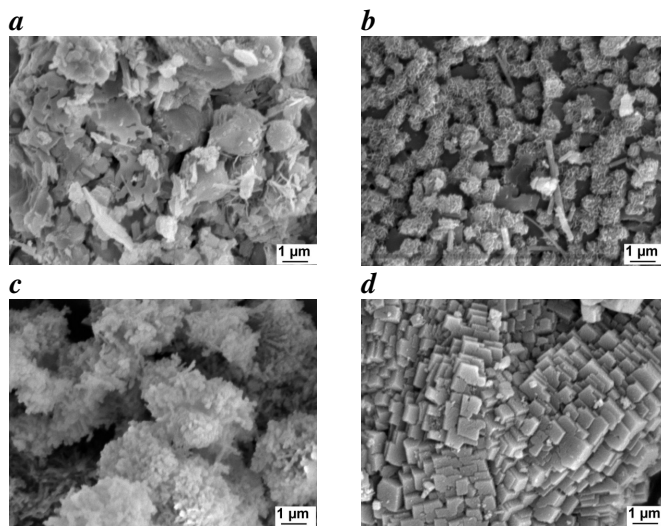Using the recirculation process water that contains an excess amount of SO_4^{2-} and/or HCO_3^--ions (RW or CRW), significantly inhibits the lime-slaking rate and the following reactions. When PF/CA ash is immersed into the carbonated recirculation water (pH ~ 7.5, $HCO_3^- = 60.75$ mmol/L; $SO_4^{2-} = 2.7$ g/L) Ca^{2+}-ion concentration in the liquid phase drops to 60–140-mg/L (see Table 13) according to the following reaction (Eq. (14)):

$$Ca^{2+} + HCO_3^- + OH^- \rightarrow CaCO_3 + H_2O \qquad (14)$$

This indicates that hydration of the lime-containing particles is already retarded.

As it was shown in Chapter 1.3.1, the presence of Ca^{2+} and OH^--ions in the slaking water decelerate the diffusion of $Ca(OH)_2$ away from the particles' surface, thus reducing the slaking rate of lime [70]. Carbonate and sulfate ions are known to form insoluble layers of both $CaCO_3$ and $CaSO_4$. These layers partially or completely coat the particles and prevent their further dissolution or slow it down [72, 73]. The SEM and EDX linescan analysis reveals that immersing ash particles into the sulfate-containing recirculation water causes the sulfur compounds (obviously in the form $CaSO_4$) to concentrate in the surface layer (Fig. 16a,b). The layer of carbonates cannot be detected by the EDX linescan analysis because the base material also contains carbon, but the solid phase analysis shows a slight increase in CO_2 percentage (1.1–1.5→2.6–3.1%, see Table 13). The small-size pores of PF ash are easily blocked although the overall SSA may increase (0.4–0.5→1.1–2.2 m^2/g; see Table 13) as a result of the precipitating reaction products ($CaSO_4$, $CaCO_3$). Surface observations also showed distinct differences between ash particles immersed into DW and CRW: instead of a hydrated surface layer formed by particle fracturing (see Fig. 15a) the cleavage of reaction products on the surface of particles seems to be more of the case (Fig. 15b).

The carbonation process decelerates shortly after introducing the CO_2-containing gas mixture into the ash–water (CRW, RW) suspension. The pH and Ca^{2+} content in the liquid phase decrease rapidly (Fig. 14a), the final product contains only 6–7% CO_2 and most of the free lime (17–18.5%) remains unreacted (Fig. 14b; Table 13). Process deceleration, which starts already during the hydration step, is the combined effect of the two factors: a low porosity of the PF ash and a high content of sulfate and/or carbonate ions in the suspension liquid phase. Due to the high concentrations of the dissolved salts in recirculation water, the diffusion of $Ca(OH)_2$ away from the surface decelerates, which, in its turn, reduces the slaking rate and causes the reactions to take place inside the pores. Insoluble layers of the precipitating reaction products easily plug the small-size pores of PF ash (see Fig. 13). The forming product layer is characterized by a crystalline and impermeable nature (Fig. 15d). Therefore, while operating with the continuous-flow reactor, the composition of the liquid phase contacted with the ash should be monitored and the production of carbonate/bicarbonate ions avoided.

Hydration of PF ash by water (PF08/CA hydr) or by the air moisture (PF07/CA*), which can be considered as a pretreatment, causes the ash particles to fracture and to disintegrate. In turn, the SSA of the ash as well as pore size

45

increases [86] and lime becomes increasingly available for the carbonation treatment (see Table 13). As a result, the aqueous carbonation process becomes less influenced by the composition of the liquid phase and the final product contains less unreacted free lime (1.97–6.97%; see Table 13).
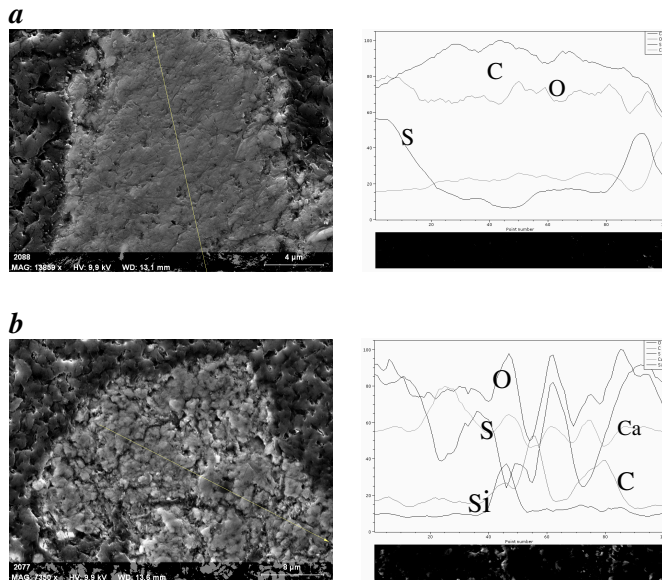
a

b

Figure 16. SEM and EDX analysis of PF ash (PF07/CA) after (a) immersing into CRW and (b) treatment with CO_2-containing model gas *(Paper IV)*

The porous structure of the CFBC ash particles supports fast and full hydration of lime as well as diffusion of Ca^{2+}-ions into solution. This results in almost complete carbonation. The outcome of carbonation does not depend on the liquid phase compositions, and the solid phase composition is almost identical to that of the systems using DW or RW (containing 16.58–16.99% of CO_2 and 1.17–1.26% of CaO_f; see Table 13). In both cases the surface is covered with a fluffy and permeable product layer *(Paper IV: Fig. 7c,d)*.

4.3.3. Continuous-flow reactor *(Paper IV)*

Continuous-mode carbonation of oil-shale waste ashes was carried out at given pre-set pH ranges. The liquid phase compositions used corresponded to the suspension pH and gave rather similar results with both types of ashes. In coordination with the high pH level of the 1st reactor, the liquid phase was oversaturated with Ca^{2+}-ions (1,100–1,500 mg/L; Fig. 17). Thus, the most suitable conditions for CO_2 absorption were created. In the case of CFBC ash, the solid phase from the 1st reactor contained 4–5% of unreacted lime and 14–16% of CO_2. This indicated that 65–70% of initial free CaO was utilized (BD_{CaO}, Fig. 18,*a*).

These indicators were somewhat lower in the case of the carbonated PF ash, which contained over 8% of unreacted lime. This shows that a 55–65-percent utilization of free CaO was achieved (BD$_{CaO}$, Fig. 18,*b*).
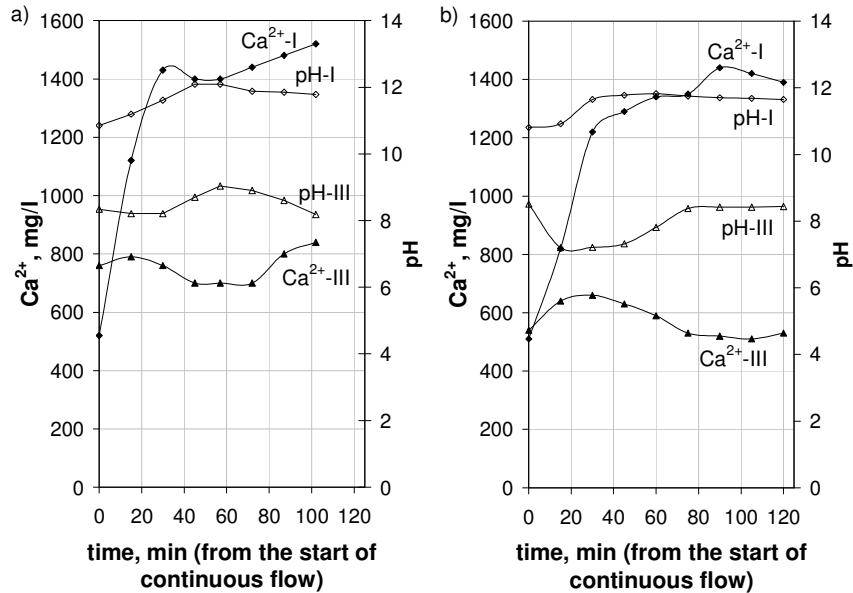

Figure 17. Changes in Ca^{2+}-ion concentrations and the pH of the suspension liquid phase during carbonation of (a) - CFBC ash and (b) - PF ash in a continuous mode *(Paper IV)*

The carbonation process was continued in the 2nd reactor, where the pH and the content of Ca^{2+}-ions in liquid phase decreased to 10–11 and 500–800 mg/L, respectively. After the 2nd reactor about 80–90% of the initial free lime was utilized. On the final stage (3rd reactor) of ash carbonation process, the suspension pH decreased to 7.5–9 and BD$_{CaO}$ stabilized on the level of 95 and 90% for CFBC ash and PF ash, respectively (Fig. 18).

Somewhat higher values of BD$_{CO2}$ (they often occurred to be over 100% in the 3rd reactor, although free lime was not completely utilized) compared to BD$_{CaO}$ showed that other potentially CO$_2$-binding components of ash, such as MgO and Ca-silicates, took part in CO$_2$-binding reactions (BD$_{CO2}$; Fig. 18,*a*). This tendency was not as apparent in the case of PF ash (Fig. 18,*b*). Although switching from tap-water to circulating process-water (pH = 8–10; Ca^{2+} = 400–700 mg/L; SO$_4^{2-}$ = 1,000–1,600 mg/L; TDS = 1.0–1.7 g/L; CO$_3^{2-}$/HCO$_3^{-}$ = 1.5–3.5 mmol/L) did not have any noticeable effect on the CFBC ash carbonation, it had a decelerating influence on the processing of PF ash (the percentage of unreacted lime increased from 1.7 to 2.9%). Evidently, in the case of PF ashes as non-porous materials [86]

47

some part of free CaO is not accessible under these conditions. The final products contained 0.6–2.9% unreacted lime and 17–20% of CO_2.
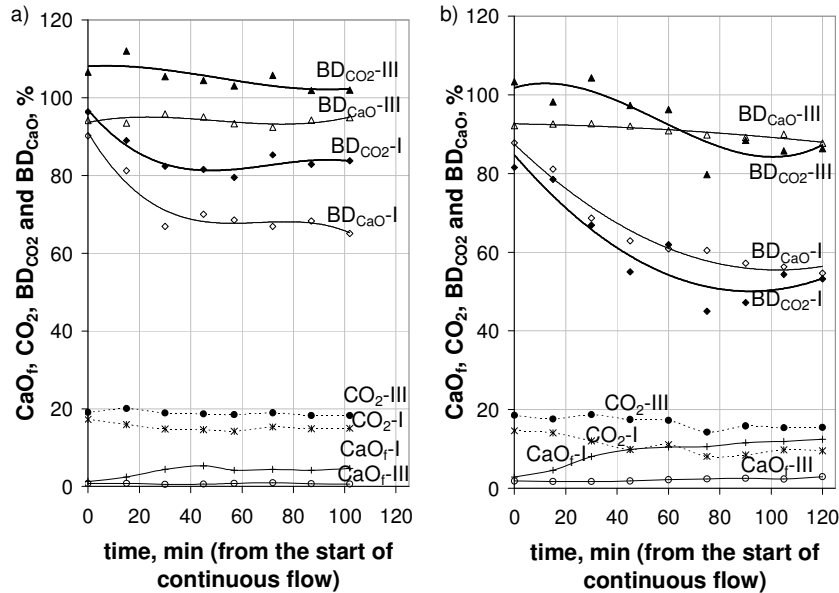

Figure 18. Changes in CaO_f and CO_2 contents and CO_2- and CaO-binding degrees during carbonation of a - CFBC and b - PF ash in continuous mode

All in all, the stability of the process of continuous-mode oil-shale waste ashes carbonation in this laboratory-scale set-up at optimal conditions was achieved for $Ca(OH)_2$ dissociation and $CaCO_3$ precipitation. The experiments confirmed significant differences in the reactivity of CFBC ash and PF ash towards CO_2. While the CFBC ash was carbonated almost completely in a continuous-flow reactor system, the PF ash probably needs a pre- or extended treatment for a deeper carbonation. The pretreatment of the pulverized-fired ash by grinding or hydration would make the free lime trapped inside the ash particles more accessible for reagents due to breaking the particles and/or increasing their porosity. Also, it is important to closely monitor the contents of sulfate and carbonate ions in the contacting liquid phase, which form insoluble product layers on the surface of particles and thereby strongly inhibit the ash-hydration process.

4.3.4. Conclusions

Experiments involving CO_2 mineral sequestration by ash–water suspensions demonstrated that both ash types qualify as effective sorbents for CO_2 capture in an aqueous mineral carbonation process, as they are able to bind 100 to 160 kg CO_2 per 1 t of ash.

Batch experiments:

- As expected, free CaO is the main CO_2-binding component in ash. But in addition to free lime, the Ca-silicates ($CaSiO_3$ and Ca_2SiO_4) and periclase should also be taken into account while calculating the maximal CO_2-binding potential of oil-shale ashes.
- Under the same conditions, CFBC ash is able to be carbonated to a greater extent compared to PF ash: BD_{CO2} values are 83–98 and 48–73%, respectively. Also, compared to PF ash, the CFBC ash can be carbonated more deeply by lowering the pH of the aqueous suspension of the solid residue, in most cases below pH = 9. In the case of non-porous PF ashes, a part of the free CaO remains unreacted and this leads to the elevated pH-values (11–12) causing environmental issues upon depositing.

Process rate-determining mechanism:

- Aqueous carbonation of PF cyclone ash, which is considered the most typical PF ash, depends to a great extent on the aqueous phase composition. In the case of the PF ash–recirculation water system, which is characterized by an excess amount of sulfate and/or carbonate ions, the process decelerates shortly after introducing the CO_2-containing model gas and most of the free lime (17–18.5%-Abs) remains unreacted.
- Process deceleration, which starts already at the hydration step, is mainly caused by concurrence of the two factors: a low porosity of PF ash and a high content of sulfate and/or carbonate ions in the liquid suspension phase. Due to the high concentration of dissolved salts in the recirculation water, the diffusion of $Ca(OH)_2$ away from the particles` surface decelerates. This, in turn, reduces the slaking rate and causes the reactions to take place inside the pores. Precipitating reaction products easily plug the small-size pores of PF ash. In the slaking water, carbonate ions and sulfate ions in form insoluble layers of both $CaCO_3$ and $CaSO_4$. These layers partially or completely coat the particle and prevent further dissolution or CaO.
- Porous structure of CFBC ash particles supports fast and full hydration of lime as well as diffusion of Ca^{2+}-ions into solution. This results in almost complete carbonation. The effect of the liquid phase composition on the slaking and diffusion rates of Ca^{2+}-ions and the following carbonation reaction is not evident.

Continuous flow experiments:

- A continuous-mode laboratory-scale reactor system for treating the oil-shale ash–water suspensions with CO_2-containing model gas was developed. The carbonation process was optimized by introducing the cascade mode of operation of the reactor-columns. The pH levels in different reactors were ranged from alkaline to almost neutral. This enabled optimal conditions for lime slaking, $Ca(OH)_2$ dissociation and $CaCO_3$ precipitation.
- The experiments confirmed significant dissimilarities in the reactivity towards CO_2 of water-suspended oil-shale ashes formed under different combustion regimes. While the CFBC ash is carbonated almost completely in the

continuous-flow reactor system, the PF ash needs pre- or extended treatment for deeper carbonation. Final products contained 0.6–2.9% wt. of unreacted lime and 17–20% wt. of bound CO_2.

4.4. CO_2 binding by alkaline ash transportation water *(Paper V)*

Intensifying the natural CO_2-binding potential of the alkaline ash-transportation water by using aeration or sprinkling technologies to bind CO_2 from the air gave moderate results [87].

Binding CO_2 from the flue gases by the alkaline ash-transportation water was discussed further in *Paper V*. The intensity of the alkaline wastewater neutralization with carbon dioxide was increased using a dispergator-type phase-mixer, a patent application was filed for the referred process [84]. The experimental setup and conditions are presented in Chapter 3.3.

4.4.1. Theoretical considerations and calculations

Large amounts (15–20 m^3 per one ton of ash) of wastewater that has a considerable CO_2-binding capacity circulate in the hydraulic ash-transportation system. A contact of Ca^{2+} ions present in the alkaline wastewater with CO_2 present in the flue gases results in the reactions described by Eqs (15) and (16):

$$Ca^{2+}(aq) + 2OH^- + CO_2(g) \rightarrow CaCO_3(s) + H_2O \qquad (15)$$

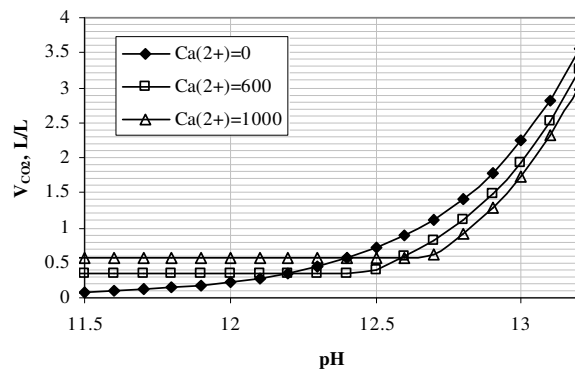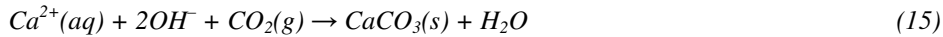$$CO_2(g) + OH^- \rightarrow HCO_3^-(aq) \qquad (16)$$

Figure 19. The amount of CO_2 needed for precipitation of Ca^{2+}-ions and neutralization of OH^--ions *(Paper V)*.

Dissolution of CO_2 into the water depends on the pH, because the forming H_2CO_3* (CO_2*H_2O) dissociates with the formation of CO_3^{2-}- and HCO_3^- -ions. Herewith,

the overall concentration of carbon C_{CO2} increases according to the amount of HCO_3^- and CO_3^{2-}-ions formed. Based on the conversion rates α showing which part of the CO_2 present in the solution goes into which particular form (CO_2, HCO_3^- or CO_3^{2-}), the dependence of the fractional amounts of all carbonate species on the solution pH is presented in Fig. 3. Around the preferable water pH value (8.5), the CO_2 is found in the solution mainly as HCO_3^-. Therefore, the fractional amount of CO_2 necessary for wastewater neutralization can be calculated according to Eq. (16).

Contact of Ca^{2+}-ions with CO_2 leads to precipitation of $CaCO_3$, which is practically insoluble in the water with pH >9. When pH >11, the solution contains mainly CO_3^{2-} ions. This means that at the beginning of the interfacial contact the $CaCO_3$ precipitation can be expected firstly (Eq. (15)). An overall CO_2 demand is calculated as the combination of CO_2 fractional amounts needed for both Ca^{2+} ions precipitation and OH^--ions neutralization (Fig. 19).

4.4.2. Comparison of the alkaline wastewater carbonation in dispergator- and barboter-type reactors

Comparative experiments with dispergator- and barboter-type reactors indicated that the alkaline ash-transportation waters (pH=13.0–13.1, Ca^{2+} content 800–1,020 mg/L) react readily with CO_2-containing model gases FG1 and FG2 decreasing the content of Ca^{2+}-ions and pH value (Fig. 20a; Table 14).

Table 14: Wastewater treatment with CO_2-and SO_2-containing model gases: composition of the solid phase and the liquid phase. (*Paper V*)

		Liquid phase						Solid phase	PCC sample
N_{CO2}	pH	TDS	Ca^{2+}	SO_4^{2-}	OH^-	CO_3^{2-}	HCO_3^-	$CaCO_3$	
		g/L			mmol/L			%	
Dispergator-type phase mixer with FG1 (CO_2 + air)									
1.5	~10	5.61	0.01	1.98	2.0	24.0	0.0	86.01	PCC1
4.5	~8	6.33	0.03	2.21	0.0	6.0	25.0	90.40	PCC2
Dispergator-type phase mixer with FG2 (CO_2 + SO_2 + air)									
1.5	~10	6.43	0.01	2.18	0.0	27.0	1.5	94.16	PCC3
4.5	~8	6.49	0.10	2.34	0.0	7.0	24.5	93.22	PCC4
Barboter-type column with FG1 (CO_2 + air)									
0.7	~10	6.30	0.005	0.96	0.0	22.5	6.5	87.95	PCC5
1.04	~8	6.54	0.135	1.20	0.0	0.0	32.5	84.77	PCC6
Barboter-type column with FG2 (CO_2 + SO_2 + air)									
0.7	~10	6.39	0.01	2.54	0.0	14.0	14.75	91.20	PCC7
1.04	~8	6.48	0.16	1.92	0.0	0.0	42.5	88.25	PCC8

In the case of a dispergator-type phase mixer, the content of Ca^{2+}-ions dropped notably – to 10 mg/L after 1 carbonation cycle (N_{CO2} = 1.5) and the pH value

decreased to the acceptable level (about 8) after 3 carbonation cycles (N_{CO_2} = 4.5). A dispergator-type reactor enhances the gas–liquid contact surface thereby promoting mass transfer rates, (Fig. 20b), but as a result of short contact time of the phases (1.25 s per cycle) dissolution of CO_2 is not completed and a higher CO_2 excess N_{CO_2} is needed (Fig. 20a) as compared to a conventional barboter-type column. Nevertheless, by using a dispergator-type reactor by a factor of up to 50 increase in specific intensity (q, $m^3/m^3 \cdot h$) calculated as the volume of processed wastewater per unit of volume of the reactor was achieved. It was found that the filtered solid samples (PCC1–PCC8, see Table 14) contained predominantly $CaCO_3$ (85–94%).
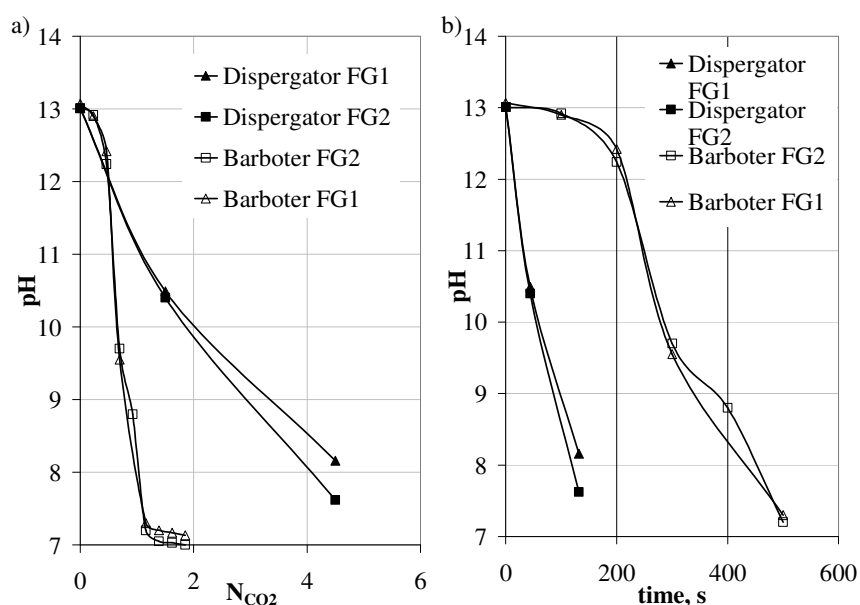
Figure 20. Changes in the wastewater pH during carbonation as a function of (a) CO_2 excess N_{CO_2} and (b) time (calculated per 1 L of wastewater) *(Paper V)*

4.4.3. Characterization of the solid product of the wastewater carbonation

PCC samples were analyzed for particle size distribution and surface properties. The results showed that the end-point pH value of the carbonation does not influence the size of PCC particles formed in the dispergator-type phase mixer (PCC1 and PCC2, *Paper V: Table 2*). The samples can be characterized by a homogeneous particle-size distribution: median size ~5 µm and mean/median ratio ~1. Presence of SO_2 in the gas mixture considerably influenced the size of the particles (PCC3 and PCC4, *Paper V: Table 2*): their median size increased noticeably due to agglomeration of particles reaching 8–9 µm. Besides this, the agglomeration effect escalated with decreasing pH. PCC4 sample was not homogeneous, containing particles in the size range 3–310 µm. The PCC samples

from the barboter-type reactor (PCC5–PCC8, *Paper V: Table 2*) had a somewhat larger particle size, which was also influenced by the extent of carbonation: median size was ~6 and 8–10 µm at pH~10 and pH~8, respectively. The presence of SO_2 had a minor influence on the size distribution characteristics of the PCC.

Shape and surface observations confirmed the results of particle-size distribution analysis. The shape of PCC particles from the dispergator-type reactor was influenced noticeably by the extent of carbonation as well as by the presence of SO_2. Regularly structured particles of PCC were formed in the high pH region in a SO_2-free environment (Fig. 21a). Extending of the carbonation process led to cleavage of the particles. In the presence of SO_2 most of the individual particles were merged, forming agglomerates (Fig. 21b).

The PCC formed in a barboter-type column is characterized by more homogeneous particles with a distinctive regular rhombohedral crystal structure as compared to the particles formed in the dispergator-type reactor. Shape and surface characteristics were not noticeably influenced by the extent of carbonation or the presence of SO_2 in the model gas (Fig. 21c).
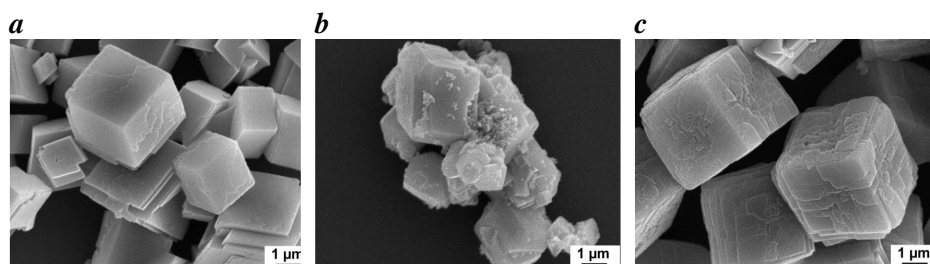

Figure 21. SEM images of the PCC samples formed at different conditions in a dispergator-type phase mixer: PCC1 (a), and PCC4 (b), and a barboter-type column: PCC8 (c)

According to thermodynamic calculations (*Paper I*), precipitation of $CaCO_3$ in the system wastewater–flue gas can be expected at the starting stages of the interfacial contact at high pH values. If pH has decreased to 7.5–9, the binding capacity of the aqueous phase is almost completely utilized and the increase in CO_2 binding is mainly due to the increase in the amount of dissolved CO_2 and formed HCO_3^-. Also, at a deeper carbonation at pH<9, $CaCO_3$ becomes more soluble in water and the concentration of Ca^{2+}-ions in the solution starts to rise again as shown in Table 14. Therefore, to avoid agglomeration of the particles and redissolution of $CaCO_3$, the alkaline wastewater neutralization process with production of PCC should be divided into two stages: first, $CaCO_3$ precipitation and separation at high pH values and second, decreasing the residual alkalinity of wastewater to acceptable levels (pH~8–8.5). Producing PCC of specific properties is a complicated process, which needs further research to obtain better understanding of the influence of different conditions on crystallization processes.

4.5. Natural CO_2 binding in ash fields *(Paper III)*

It was shown that the most intensive CO_2 binding takes place in the surface layers within a few centimeters; while in the deeper layers the binding rate is moderate. Pile-up of fresh layers of ash suspension inhibits CO_2 diffusion into the deeper layers and CO_2 binding reactions.

Summer temperature conditions enhance the natural binding of CO_2 into the surface layers of ash deposits, while surrounding temperature does not influence the process in the deeper layers remarkably. Autumn/spring and winter conditions greatly inhibit the rate and extent of the processes under discussion giving prerequisites for chemical reactions and mass/heat transfer.

Table 15: CO_2-binding characteristics of different types of oil-shale ash in natural conditions (average results from experiments in summer, spring/autumn and winter conditions), *% (Paper III)*

Time, weeks	CFBCA				PFA				CFBC and PFA mixture, 1:1			
	ΔCO_2		BD		ΔCO_2		BD		ΔCO_2		BD	
	1. layer	1-6. layers	1. layer	1-6. layers	1. layer	1-6. layers	1. layer	1-6 layers	1. layer	1-6. layers	1. layer	1-6. layers
0	0	0	0	0	0	0	0	0	0	0	0	0
1	3.33	2.98	62.2	55.9	0.89	0.28	7.9	2.5	1.71	1.39	21.2	17.3
2	4.02	3.06	74.7	57.4	1.40	0.48	12.3	4.2	2.14	1.37	26.5	16.9
4	4.55	3.11	82.6	57.5	2.20	0.54	19.0	4.5	3.41	1.89	42.3	23.4
8	5.75	3.12	105.4	58.2	3.48	0.89	30.5	7.7	5.22	2.19	64.7	27.1

Comparison of different kinds of ashes showed that CFBC ashes react readily with atmospheric CO_2, but their total binding capacity is quite low due to only moderate contents of free CaO. Therefore, a substantial part (60-80%) of the CO_2 binding capacity of the CFBC ash could be exhausted at natural conditions (Table 15). In the case of PF ash, which is characterized by a considerable CO_2-binding potential as well as by a low surface area of the particles, most of the free CaO present in the initial ash remains unrealized at given time periods – the average value of BD was within 4.5% after 1 month of deposition (Table 15). Differences in the reactivity of ashes are related to the structure and surface properties of the ash particles (*Paper II*): for instance the SSA of the CFBC ashes is up to ten times that of the PF ashes.

Considering the average results of experiments in model conditions (Table 15), 1 ton of ash binds 9–31 kg CO_2, giving an average of ~100,000 t CO_2 bound by open-air ash deposits annually at the production level of 2006.

4.6. Technological evaluation and expected amounts of CO_2 bound

This study demonstrates that the total amount of naturally-bound CO_2 can reach 52 kg CO_2 per 1 t ash (Table 16). The amount of CO_2 bound by a 1:1 mixture of CFBC ash and PF ash under the natural storage conditions is ca. 22 kg/t.

54

Implementation of the simple and inexpensive technical methods [87] could double this amount (up to 44 kg/t).

In laboratory experiments, the amount of CO_2 bound by direct carbonation of ash-mixture suspensions with model gases varied from 100 to 160 kg CO_2/t ash depending on the ash type. The average quantity bound was 140 kg/t, which is equivalent to 7.3% of the total and 43.6% of the carbonaceous CO_2 emission, respectively. Application of the above-mentioned methods would radically decrease the remaining content of CO_2-active compounds in the ash. Additional research is necessary to estimate the potential amount of CO_2 that can be bound by the carbonated ash in open-air deposits. We presume that the total amount of CO_2 bound (during carbonation and consequent deposition) would be similar to the sum of CO_2 bound by the direct carbonation of ash–water suspension and water neutralization (192–209 kg/t ash or 10–11% and 60–65% of the total and mineral carbon content, respectively).

Table 16: The amount of CO_2 (A, 10^3 t) bound per 1 million t ash and the ratio (B, %) of the total amount (in numerator) to the mineral part (in denominator) of CO_2 emitted at oil-shale combustion *(Paper III)*

No	CO_2-binding	Natural open-air binding		Technological abatement	
		A	B	A	B
1.	By circulating water				
1.1.	Ca^{2+} partial precipitation (in natural conditions)	8.4	0.4/2.6		
1.2.	Ca^{2+} full precipitation [87]			16.0	0.8/5.0
1.3.	Ca^{2+} precipitation + neutralization (laboratory experiments)			52.0	2.7/16.2
2.	By ash deposits				
2.1.	PF ashes according to [87]	24.8	1.3/7.7	49.6	2.6/15.4
2.2.	Mixture of PF ash and CFBC ash, 1:1	22.0	1.1/6.9	44.0	2.3/13.7
	Total natural binding, sum of positions 1 and 2.2	30.4	1.6/9.5		
	Total natural binding with simple technological measures [87]			60.0	3.1/18.7
3.	By carbonation of ash suspensions				
3.1.	Results of laboratory experiments			140	7.3/43.6
	Sum of positions 1.3 and 3.1			192	10.0/59.8
3.2.	Results of calculations				
3.2.1.	20% of CaO_{total} utilized			157	8.2/49.9
3.2.2	30% of CaO_{total} utilized			236	12.3/73.5
	Sum of positions 1.3. and 3.2.1			209	10.9/65.1

The main considerations and the initial data for a design of an industrial pilot-scale plant have been defined and compiled and the principal flow-sheet has been proposed (*Paper IV: Fig. 11*). Considering the real production output, for example

at the Narva Power Plant, it is reasonable to choose the capacity of the test plant to be 120 t/h ash (the capacity of one ash-removal section). The solid : liquid ratio of the pulp to be processed is 1 : 10 which is suitable according to the experiments reprinted here. To guarantee a higher flexibility of the process, it is reasonable to divide the total capacity of the test device over several lines. In the case of four lines, the capacity of one line will be 30 t per hour and the total volume of the reactors will then be approximately 300 m^3.

A few important aspects should be taken into account when designing a pilot-scale plant:

- The suspension pH value was chosen to be the main indicator to control the chemical conversion progress. To ensure the optimal conditions for lime slaking and dissociation of Ca^{2+}-ions into the bulk solution, the pH values should be carefully chosen for all the reactors composing the line and also optimized during exploitation of the plant.
- To decrease the suspension pH to the optimum final level 8.5 ± 0.3 at the capacity of one line at 30 t/h, it is necessary to introduce 20,000 (at stoichiometric ratio $N_{CO2} = 1.0$–1.2) to 30,000 m^3/h ^{STP} ($N_{CO2} = 1.5$) of flue gases (content of CO_2 15% vol.).
- Gas-injection density was recommended as the main factor determining the reactor dimensions (suspension-column height and reactor diameter). An initial value of 100 m^3/m^2*h could be recommended by adjusting the results of the laboratory experiments to a 3–5 times increase in the liquid column height.
- The construction and working regimes of stirrers should be chosen carefully to avoid passive zones at the reactor-column bottom. Also, a smooth-running suspension flow between the reactors should be provided.
- Rotating impellers should avoid the gravity settling of the solid phase and at the same time slow down the vertical movement of gas bubbles. The inlet of flue gases should be placed as deep as possible as to guarantee the maximal and homogeneous interfacial contact (a possible inlet of gas phase is through stirrer shaft and impellers).
- Considering the large volumes of gas–liquid flows, the exiting gases should be passed through a droplet separator, or "de-mister". As the process involves alkaline Ca^{2+}-ion-containing solutions and CO_2-containing gases, precipitation in the gas inlet and outlet sections and equipments is highly probable and therefore a periodical high-pressure cleaning is required.

5. CONCLUSIONS

Waste ashes from the oil shale combustion have been characterized as sorbents for CO_2 binding from the flue gases in aqueous mineral carbonation processes. The CO_2 binding potential of various oil-shale ash components has been evaluated. CO_2 emissions from the Estonian oil shale-based power production could be diminished using the waste ash as CO_2 sorbent: the total fractional amount of CO_2 bound (during the carbonation and consequent deposition) averaged to 192–209 kg/t ash or 10–11% and 60–65% of the total and mineral carbon content, respectively.

1. The behavior of lime as the key component of the ash in various conditions was elaborated and the mechanism of process deceleration proposed.
2. The concept of CO_2 mineral sequestration in the oil-shale waste ashes from Estonian power production has been proposed as a way to mitigate the release of the greenhouse gases formed by the burning of fossil fuel oil shale into the atmosphere.
3. The main parameters for the aqueous processes of CO_2 binding – via direct (ash suspensions) or indirect (ash-transportation water) aqueous carbonation of the ash with flue gases and via a natural weathering – have been elaborated. The results can serve as the initial data for an industrial-scale pilot plant design.
4. A new method for the neutralization of the alkaline Ca^{2+}-containing wastewater using carbon dioxide from the flue gas has been worked out. It was shown that alkaline ash-transportation water could be considered as a resource for the production of PCC characterized by a regular rhombohedral structure and a homogeneous particle size (~5μm) distribution.

REFERENCES

1.   *IPCC Special Report on Carbon Dioxide Capture and Storage*; Intergovernmental Panel of Climate Change: Cambridge University Press, Cambridge, United Kingdom and New York, USA, 2005; p 443 p.

2.   Kasvuhoonegaaside heitkoguste vähendamise riiklik programm aastateks 2003-2012. http://www.keskkonnainfo.ee/failid/kliimaveeb/20a.pdf

3.   Rao, A. B.; Rubin, E. S., A Technical, Economic, and Environmental Assessment of Amine-Based CO_2 Capture Technology for Power Plant Greenhouse Gas Control. *Environmental Science and Technology* **2002,** *36*, 4467-4475.

4.   Franco, A.; Diaz, A. R. In *Environmental sustainability of CO_2 capture in fossil fuel power plants*, Ecosystems and Sustainable Development VI, Coimbra, Portugal, 2007; Brebbia, C., Ed. WIT Press: Coimbra, Portugal, 2007; pp 251-261.

5.   Holloway, S., Underground sequestration of carbon dioxide - a viable greenhouse gas mitigation option. *Energy* **2005,** *30*, 2318-2333.

6.   Huijgen, W. J. J.; Comans, R. N. J.; Witkamp, G.-J., Cost evaluation of CO_2 sequestration by aqueous mineral carbonation. *Energy Conversion and Management* **2007,** *48*, 1923-1935.

7.   Seifritz, W., CO_2 disposal by means of silicates. *Nature* **1990,** *345*, 486.

8.   Dunsmore, H. E., A geological perspective on global warming and the possibility of carbon dioxide removal as calcium carbonate mineral. *Energy Conversion and Management* **1992,** *38*, 259-264.

9.   Lackner, K. S.; Wendt, C. H.; Butt, D. P.; Joyce, E. L.; Sharp, D. H., Carbon disposal in carbonate minerals. *Energy* **1995,** *20*, 1153-1170.

10.   Lackner, K. S.; Butt, D. P.; Wendt, C. H., Progress of binding CO_2 in mineral substrates. *Energy Conversion and Management* **1997,** *38*, 259-264.

11.   Lackner, K. S., Carbonate chemistry for sequestrating fossil carbon. *Annual Review of Energy and Environment* **2002,** *27*, 193-232.

12.   Lackner, K. S., A guide to CO_2 sequestration. *Nature* **2003,** *300*, 1677-1678.

13.   Huijgen, W. J. J.; Comans, R. N. J. *Carbon dioxide sequestration by mineral carbonation*; Energy Research Centre of The Netherlands: Petten, The Netherlands, 2005.

14.   Sipilä, J.; Teir, S.; Zevenhoven, R. *Carbon dioxide sequestration by mineral carbonation Literature review update 2005–2007*; Report 2008-1; Abo Akademi University, Faculty of Technology, Heat Engineering Laboratory: 2008.

15.   O`Connor, W. K.; Dahlin, D. C. In *CO_2 storage in solid form: a study of direct mineral carbonation*, 5-th International Conference on Greenhouse Gas technologies, Cairns, Australia, 2000; Cairns, Australia, 2000.

16.   O`Connor, W. K.; Dahlin, D. C.; Nilsen, D. N.; Rush, G. E.; Walters, R. P.; Turner, P. C. In *Carbon dioxide sequestration by mineral carbonation: results from recent studies and current status*, Proceedings of the First National

Conference on Carbon Sequestration, Washington DC, USA, May 14-17, 2001; Washington DC, USA, 2001.

17.   Gerdemann, S. J.; Dahlin, D. C.; O`Connor, W. K.; Penner, L. R.; Rush, G. E. In *Factors Affecting Ex-situ Aqueous Mineral Carbonation Using Calcium and Magnesium Minerals*, The Proceedings of the 29-th International Conference on Coal Utilization and Fuel Systems, Clearwater, Florida, USA, 18-22 April, 2004; Sakkestad, B. A., Ed. Coal Technology Association: Clearwater, Florida, USA, 2004.

18.   Haywood, H. M.; Eyre, J. M.; Scholes, H., Carbon dioxide sequestration as stable carbonate minerals - environmental barriers. *Environmental Geology* **2001,** *41*, 11-16.

19.   Costa, G.; Baciocchi, R.; Polettini, A.; Pomi, R.; Hills, C. D.; Carey, P. J., Current status and perspectives of accelerated carbonation processes on municipal waste combustion residues. *Environ Monitoring Assess* **2007,** *135*, 55-75.

20.   Baciocchi, R.; Polettini, A.; Pomi, R.; Prigiobbe, V.; Von Zedwitz, V.; Steinfeld, A., CO_2 Sequestration by Direct Gas-Solid Carbonation of Air Pollution Control (APC) Residues. *Energy and Fuels* **2006,** *20*, 1933-1940.

21.   Stolaroff, J. K.; Lowry, G. V.; Keith, D. W., Using CaO and MgO-rich waste streams for carbon sequestration. *Energy Conversion and Management* **2005,** *46*, 687-699.

22.   Huijgen, W. J. J.; Comans, R. N. J., Carbonation of Steel Slag for CO_2 Sequestration: Leaching of Products and Reaction Mechanisms. *Environmental Science and Technology* **2006,** *40*, (2790-2796).

23.   Huijgen, W. J. J.; Witkamp, G.-J.; Comans, R. N. J., Mineral CO_2 Sequestration by Steel Slag Carbonation. *Environmental Science and Technology* **2005,** *39*, 9676-9682.

24.   Teir, S.; Eloneva, S.; Fogelholm, C.-J.; Zevenhoven, R., Dissolution of steelmaking slags in acetic acid for precipitated calcium carbonate production. *Energy* **2007,** *32*, 528-539.

25.   Fernández Bertos, B.; Simons, S. J. R.; Hills, C. D.; Carey, P. J., A review of accelerated carbonation technology in the treatment of cement-based materials and sequestration of CO_2. *Journal of Hazardous Materials* **2004,** *B112*, 193-205.

26.   Rendek, E.; Ducom, G.; Germain, P., Carbon dioxide sequestration in municipal solid waste incinerator (MSWI) bottom ash. *Journal of Hazardous Materials* **2006,** *B128*, 73-79.

27.   Zevenhoven, R.; Kavaliauskaite, I., Mineral carbonation for long-term CO_2 storage: and exergy analysis. *International Journal of Thermodynamics* **2004,** *7*, 22-31.

28.   Baciocchi, R.; Polettini, A.; Pomi, R.; Prigiobbe, V.; Zedtwitz-Nikulshyna, V.; Steinfeld, A. In *Performance and kinetics of CO_2 sequestration by direct gas-solid carbonation of APC residues*, 8-th International Conference of Greenhouse Gas Control Technologies, Trondheim, Norway, 17-22 June, 2006; Elsevier ltd: Trondheim, Norway, 2006; pp 5 p. on CD-ROM.

29.   O`Connor, W. K.; Dahlin, D. C.; Rush, G. E.; Gerdemann, S. J.; Penner, L. R. In *Energy and economic considerations for ex-citu aqueous mineral carbonation*, The Proceedings of the 29-th International Technical Conference on Coal Utilization and Fuel Systems, Clearwater, Florida, USA, April 18-22, 2004; Sakkestad, B. A., Ed. Coal Technology Association: Clearwater, Florida, USA, 2004.

30.   Munz, I. A.; Korneliussen, A.; Gorset, O.; Johansen, H.; Kihle, J.; Flaathen, T.; Sandvik, K. In *Added value of industrial minerals and CO_2 storage: New possibilities for Norwegian mineral industry*, 8-th International Conference of Greenhouse Gas Control Technologies, Trondheim, Norway, 17-22 June, 2006; Elsevier ltd: Trondheim, Norway, 2006; pp 5 p. on CD-ROM.

31.   Gerdemann, S. J.; O`Connor, W. K.; Dahlin, D. C.; Penner, L. R.; Rush, H., Ex Situ Acueous Mineral Carbonation. *Environmental Science and Technology* **2007,** *41*, 2587-2593.

32.   Huijgen, W. J. J.; Witkamp, G.-J.; Comans, R. N. J., Mechanisms of aqueous wollastonite carbonation as a possible CO_2 sequestration process. *Chemical Engineering Science* **2006,** *61*, 4242-4251.

33.   Maroto-Valer, M. M.; Fauth, D. J.; Kuchta, M. E.; Zhang, Y.; Andresen, J. M., Activation of magnesium rich minerals as carbonation feedstock materials for CO2 sequestration. *Fuel Processing Technology* **2005,** *86*, 1627-1645.

34.   Park, A. A.-H.; Fan, L.-S., CO_2 mineral sequestration: physically activated dissolution of serpentine and pH swing process. *Chemical Engineering Science* **2004,** *59*, (22-23), 5241-5247.

35.   McKelvy, M. J.; Chizmeshya, A. V. G.; Diefenbacher, J.; Bearat, H.; Wolf, G., Exploration of the role of heat activation in enhancing serpentine carbon sequestration reactions. *Environmental Science and Technology* **2004,** *38*, 6897-6903.

36.   Huijgen, W. J. J.; Comans, R. N. J. *Carbon dioxide sequestration by mineral carbonation: Literature review. ECN-C-03016*; ECN-C-03-016; Energy Research Centre of the Netherlands: 2003.

37.   Van Gerven, T.; Van Keer, E.; Arickx, S.; Jaspers, M.; Wauters, G.; Vandecasteele, C., Carbonation of MSWI-bottom ash to decrease heavy metal leaching, in view of recycling. *Waste Management* **2005,** *25*, 291-300.

38.   Meima, J. A.; van der Weijden, R. D.; Eighmy, T. T.; Comans, R. N. J., Carbonation processes in municipal solid waste incinerator bottom ash and their effect on the leaching of copper and molybdenum. *Applied Geochemistry* **2002,** *17*, 1503-1513.

39.   Li, X.; Fernandez Bertos, M.; Hills, C. D.; Carey, P. J.; Simon, S., Accelerated carbonation of municipal solid waste incineration fly ashes. *Waste Management* **2007,** *27*, 1200-1206.

40.   Kuusik, R.; Veskimäe, H.; Uibu, M., Carbon dioxide binding in the heterogeneus systems formed at combustion of oil shale. 3. Transformations in the system suspension of ash - flue gases. *Oil Shale* **2002,** *19*, (3), 277-288.

41.   Jia, L.; Anthony, E. J., Pacification of FBC ash in a pressurized TGA. *Fuel* **2000,** *79*, 1109-1114.

42.   Anthony, E. J.; Bulewicz, E. M.; Dudek, K.; Kozak, A., The long term behaviour of CFBC ash–water systems. *Waste Management* **2002,** *22*, 99-111.

43.   Kuusik, R.; Uibu, M.; Toom, M.; Muulmann, M.-L.; Kaljuvee, T.; Trikkel, A., Sulphation and carbonization of oil shale CFBC ashes in heterogeneous systems. *Oil Shale* **2005,** *22*, (4 Special), 421-434.

44.   Van Balen, K., Carbonation reaction of lime, kinetics at ambient temperature. *Cement and Concrete Research* **2005,** *35*, 647-657.

45.   Ots, A., *Põlevkivi põletustehnika*. Tallinn, 2004.

46.   Fernández Bertos, M.; Li, X.; Simons, S. J. R.; Hills, C. D.; Carey, P. J., Investigation of accelerated carbonation for the stabilisation of MSW incinerator ashes and the sequestration of CO_2. *Green Chemistry* **2004,** *6*, 428-436.

47.   Kodama, S.; Nishimoto, T.; Yogo, K.; Yamada, K. In *Design and evaluation of a new CO_2 fixation process using alkaline-earth metal wastes*, 8-th International Conference of Greenhouse Gas Control Technologies, Trondheim, Norway, 19-22 June, 2006; Elsevier ltd.: Trondheim, Norway, 2006; pp 5 p. on CD-ROM.

48.   Reddy, K. J.; Gloss, S. P.; Wang, L., Reaction of CO_2 with alkaline solid wastes to reduce contaminant mobility. *Water Research* **1994,** *28*, (6), 1377-1382.

49.   Polettini, A.; Pomi, R., The leaching behavior of incinerator bottom ash as affected by accelerated ageing. *Journal of Hazardous Materials* **2004,** *B113*, 209-215.

50.   Arickx, S.; Van Gerven, T.; Vandecasteele, C., Accelerated carbonation for treatment of MSWI bottom ash. *Journal of Hazardous Materials* **2006,** *B137*, 235-243.

51.   Cornelis, G.; Van Gerven, T.; Vandecasteele, C., Antimony leaching from uncarbonated and carbonated MSWI bottom ash. *Journal of Hazardous Materials* **2006,** *A137*, 1284-1292.

52.   Dijkstra, J. J.; Van Zomeren, A.; Meeussen, J. C. L.; Comans, R. N. J., Effect of Accelerated Aging of MSWI Bottom Ash on the Leaching Mechanisms of Copper and Molybdenum. *Environmental Sience and Technology* **2006,** *40*, (14), 4481-4487.

53.   Todorovic, J.; Ecke, H., Demobilisation of critical contaminants in four typical waste-to-energy ashes by carbonation. *Waste Management* **2006,** *26*, (4), 430-441.

54.   Astrup, T.; Rosenblad, C.; Trapp, S.; Christensen, T. H., Chromium Release from Waste Incineration Air-Pollution-Control Residues. *Environmental Science and Technology* **2005,** *39*, (9), 3321-3329.

55.   Ecke, H., Sequestration of metals in carbonated municipal solid waste incineration (MSWI) fly ash. *Waste Management* **2003,** *23*, 631-640.

56.   Zevenhoven, R.; Eloneva, S.; Teir, S. In *A study on MgO-based mineral carbonation kinetics using pressurised thermo-gravimetric analysis*, 8-th

International Conference of Greenhouse Gas control Technologies, Trondheim, Norway, 19-22 June 2006; Elsevier ltd: Trondheim, Norway, 2006.

57.   Zevenhoven, R.; Teir, S. In *Long-term storage of CO_2 as magnesium carbonate in Finland*, 3rd Annual Conference on Carbon Capture and Sequestration Alexandria (VA), May 3-6, 2004; Alexandria (VA), 2004.

58.   Kakizawa, M.; Yamasaki, A.; Yanagisawa, Y., A new CO_2 disposal process via artificial weathering of calcium silicate accelerated by acetic acid. *Energy* **2001,** *26*, 341-354.

59.   Bearat, H.; McKelvy, M. J.; Chizmeshya, A. V. G.; Gormley, D.; Nunez, R.; Carpenter, R. W.; Squires, K.; Wolf, G., Carbon sequestration via aqueous olivine mineral carbonation: Role of passivationg layer formation. *Environmental Science and Technology* **2006,** *40*, 4802-4808.

60.   Park, A. A.-H.; Jadhav, R.; Fan, L.-S., Mineral sequestration: chemically enhanced aqueous carbonation of serpentine. *Canadian Journal of Chemical Engineering* **2003,** *81*, (3-4), 885-890.

61.   Blencoe, J. G.; Palmer, D. A.; Anovitz, L. M.; Beard, J. S. Carbonation of metal silicates for long-term CO_2 sequestration. US20040213705, 2004.

62.   Teir, S.; Eloneva, S.; Zevenhoven, R., Production of precipitated calcium carbonate from calcium silicates and carbon dioxide. *Energy Conversion and Management* **2005,** *46*, 2954-2979.

63.   Zevenhoven, R.; Eloneva, S.; Teir, S., Chemical fixation of CO_2 in carbonates: Routes to valuable products and long-term storage. *Catalysis Today* **2006,** *115*, 73-79.

64.   Katsuyama, Y.; Yamasaki, A.; Iizuka, A.; Fujii, M.; Kumagai, K.; Yanagisawa, Y., Development of a process for producing high-purity calcium carbonate ($CaCO_3$) from waste cement using pressurized CO_2. *Environmental Progress* **2005,** *24*, (2), 162-170.

65.   Teir, S.; Kuusik, R.; Fogelholm, C.-J.; Zevenbergen, C., Production of magnesium carbonates from serpentinite for long-term storage of CO_2. *International Journal of Mineral Processing* **2007,** *85*, 1-15.

66.   Geerlings, J. J. C.; Van Mossel, G. A. F.; Int Veen, B. C. M. Process for sequestration of carbon dioxide. WO2007071633, 18. Dec., 2006.

67.   Garcia-Carmona, J.; Gomez-Moarles, J.; Rodriguez-Clemente, R., Morphological control of precipitated calcite obtained by adjusting the electrical conductivity in the $Ca(OH)_2$-H_2O-CO_2 system. *Crystal Growth* **2003,** *249*, 561-571.

68.   Domingo, C.; Loste, E.; Gomez-Morales, J.; Garcia-Carmona, J., Calcite precipitation by high-pressure CO_2 carbonation route. *The Journal of Supercritical Fluids* **2006,** *36*, 202-215.

69.   Boynton, R. S., *Chemistry and Technology of Lime and Limestone*. Second Edition ed.; John Wiley and Sons Inc: New York, 1980; p 563.

70.   Ritchie, I. M.; Xu, B.-a., The kinetics of lime slaking. *Hydrometallurgy* **1990,** *23*, (2-3), 377-396.

71.   Giles, D. E.; Ritchie, I. M.; Xu, B.-a., The kinetics of dissolution of slaked lime. *Hydrometallurgy* **1992,** *32*, (1), 119-128.

72.   Xu, B.; Giles, D. E.; Ritchie, I. M., Reaction of lime with carbonate containing solutions. *Hydrometallurgy* **1998,** *48*, (2), 205-224.

73.   Potgieter, J. H.; Potgieter, P. P.; de Waal, D., An empirical study of factors influencing lime slaking Part II: Lime constituents and water composition. *Water SA* **2003,** *29*, (2), 157-161.

74.   Lower, S. K., Carbonate equilibria in natural waters. In *A Chem1 Environmental Chemistry*, 1999.

75.   Van Gerven, T.; Moors, J.; Dutre, V.; Vandecasteele, C., Effect of CO_2 leaching from a cement-stabilized MSWI fly ash. *Cement and Concrete Research* **2004,** *34*, 1103-1109.

76.   Garcia-Carmona, J.; Gomez-Morales, J.; Rraile-Sainz, J.; Rodriguez-Clemente, R., Morphological characteristics and aggregation of calcite crystals obtained by bubbling CO_2 through a $Ca(OH)_2$ suspension in the presence of additives. *Powder Technology* **2003,** *130*, 307-315.

77.   *Greenhouse gas emissions in Estonia 1990-2005. National Inventory report to the UNFCCC secretariat*; Ministry of the Environment: Tallinn, 2007.

78.   *Estonia`s Third National Communication under the UN Framework Convention on Climate Change*; Ministry of the Environment: Tallinn, 2001.

79.   Kallaste, T.; Liik, O.; Ots, A., *Possible energy sector trends in Estonia. Context of Climate Change*. Stockholm Environment Institute Tallinn Centre: Tallinn, 1999; p 180.

80.   *Outokumpu HSC Chemistry for Windows. Cchemical Reaction and Equilibrium Software with Extensive Thermochemical database. Version 4.0. License Ser. No. 40050 for Tallinn University of Technology.*

81.   Reispere, H. J., Determination of free CaO content in oil shale ash. *Transact. Tallinn Polytechnical Institute, series A. Nr. 245* **1966**, 73-76.

82.   Taylor, J. C., Computer programs for standardless quantitative analysis of minerals using the full powdered diffraction profile. *Powder Diffraction* **1991,** *6*, 2-9.

83.   Colin, R. W.; Taylor, C. J.; Cohen, D. R., Quantitative mineralogy of andstones by X-Ray diffractometry and normative analysis. *Journal of Sedimentary Research* **1999,** *69*, 1050-1062.

84.   Kuusik, R.; Uus, M.; Uibu, M.; Stroganov, G.; Parts, O.; Trikkel, A.; Pepoyan, V.; Terentiev, A.; Kalnapenk, E. Method for neutralization of alkaline waste water with carbon doxide consisting in flue gas. Patent application EE200600041, 22.12.2006, 2006.

85.   Kuusik, R.; Uibu, M.; Trikkel, A. In *CO_2 emission in Estonian oil shale based energy sector - prospects for abatement by wet mineral carbonization*, 8-th International Conference on Greenhouse Gas Technologies, Trondheim, Norway, 17-22 June, 2006; Elsevier ltd.: Trondheim, Norway, 2006; pp 5p. on CD-ROM.

86.   Uibu, M.; Trikkel, A.; Kuusik, R. In *Transformations in the solid and liquid phase at aqueous carbonization of oil shale ash*, Proc. ECOSUD VI, 4-7

Sept. 2007, Coimbra, Portugal, 2007; WIT Transactions on Ecology and Environment: 4-7 Sept. 2007, Coimbra, Portugal, 2007; pp 473-483.
87.   Kuusik, R.; Veskimäe, H.; Kaljuvee, T.; Part, O., Carbon dioxide binding in the heterogeneous systems formed by combustion of oil shale 1. Carbon dioxide binding at oil shale ash deposits. *Oil Shale* **2001,** *18*, (2), 109-122.

ABSTRACT

Emissions of greenhouse gases and the safe deposition/utilization of solid wastes are among most serious problems caused by extensive usage of low-grade solid fuels in the world heat-and-power production. CO_2 sequestration by mineral carbonation using alkaline waste residues serves both causes, as after stabilization by accelerated carbonation, the leaching behavior of the alkaline waste materials is often improved.

In the Republic of Estonia, a local low-grade carbonaceous fossil fuel Estonian oil shale is used as a primary energy source. Combustion of oil shale is characterized by high specific carbon emissions because of the high content of mineral carbonates present in the oil shale. In Estonia, the power sector is the largest CO_2 emitter and is also a source of huge amounts of waste ash. Depending on the combustion technology (PF or CFBC), the ash contains a total of up to 30%-wt free Ca-Mg oxides. By using CO_2 from the flue gases as a neutralizing agent, the emission of CO_2 could be diminished.

The aims of the current study were to measure the CO_2-binding ability of the waste ashes at different stages of its transportation and under different deposition conditions and to establish a concept for abatement of the CO_2 emissions in Estonian oil shale-based power production via chemical and technological methods.

The results indicated that the waste ash from the oil shale combustion qualifies as effective sorbent for CO_2 capture in aqueous mineral carbonation processes. Model experiments demonstrated that free CaO is the main CO_2-binding component in the ash. However, in addition to free lime, the Ca-silicates ($CaSiO_3$ and Ca_2SiO_4) and periclase should also be taken into account while calculating the maximal CO_2-binding potential of the oil-shale ash.

The behavior of lime as the key component of the ash in various conditions was also elaborated and the rate-determining mechanism was identified. It was found that the PF ash, which is characterized by low porosity and small size pores is especially affected by the process deceleration. Due to a high concentration of the dissolved salts in the recirculation water, the diffusion of $Ca(OH)_2$ away from the particle`s surface decelerates, which, in its turn, reduces the slaking rate and causes the reactions to take place inside the pores. Precipitation of the reaction products such as $CaCO_3$ and $CaSO_4$ may partially or completely coat the particle and prevent the further dissolution or CaO. The porous structure of the CFBC ash particles supports a fast and full hydration of lime as well as the diffusion of Ca^{2+}-ions into a solution, and this results in an almost complete carbonation.

The concept of the CO_2 mineral sequestration in the oil-shale waste ashes from Estonian power production has been proposed as a way to mitigate the accumulation of greenhouse gases released by the burning of a fossil fuel, oil shale in the atmosphere. The main parameters for aqueous processes of CO_2 binding – via direct (ash suspensions) or indirect (ash-transportation water) aqueous carbonation of the ash with flue gases and via natural weathering – were

elaborated. The results can serve as initial data for an industrial-scale pilot plant design.

A new method for the neutralization of an alkaline Ca^{2+}-containing wastewater with carbon dioxide present in the flue gas has been worked out. It was shown that the alkaline ash-transportation water could be considered as a source for production of precipitated calcium carbonate (PCC) characterized by a regular rhombohedral structure and homogeneous particle-size (~5µm) distribution.

CO_2 emissions from the Estonian oil shale-based power production could be diminished significantly using the waste ash as CO_2 sorbent: the total fractional amount of CO_2 bound (during the carbonation and consequent deposition) averaged 192–209 kg/t ash or 10–11% and 60–65% of the oil shale's total and mineral carbon content, respectively.

KOKKUVÕTE

Madala kütteväärtusega tahkkütuste põletamine energia tootmiseks tekitab mitmeid keskkonnakaitselisi probleeme nagu kasvuhoonegaaside emissioon atmosfääri ja tahke põletusprodukti ohutu ladustamine. Aluseliste jäätmete kasutamine CO_2 mineraliseerimiseks annab mitmese keskkonnakaitselise efekti, vähendades samaaegselt nii CO_2 emissiooni kui ka ladustatava jääkprodukti keskkonnaohtlikkust.

Eestis emiteeritavast süsihappegaasi hulgast pärineb suurem osa energeetikasektorist, mille põhitoormeks on põlevkivi. Põlevkivil on võrreldes teiste kütustega suurem süsinikuemissiooni koefitsient tema kõrge mineraalse CO_2 ehk karbonaatide sisalduse tõttu. Olenevalt põletamistehnoloogiast sisaldab tekkiv tuhk kuni 30% karbonaatide termilisel lagunemisel tekkivaid Ca- ja Mg-oksiide. Põlevkivi põletamisel tekkiva CO_2 sidumine tuha leeliseliste komponentidega võimaldab vähendada nii atmosfääri saastava CO_2 emissiooni kui ka ladustatava tuha keskkonnaohtlikkust.

Antud töö ülesandeks oli hinnata tuha CO_2 sidumisvõimekust erinevates transpordietappides ja ladustamistingimustes ning koostada kontseptsioon CO_2 emissiooni piiramiseks Eesti põlevkivienergeetikas keemilis-tehnoloogiliste vahenditega.

Tulemused näitasid, et põlevkivi tolm- ning keevkihtpõletamisel formeeruvad tuhad on oma koostise ning omaduste poolest sobivad sorbendid sidumaks CO_2 samas tekkivatest suitsugaasidest. Mudelkatsete põhjal on tuha kõige aktiivsemaks komponendiks kaltsiumoksiid, kuid tuha CO_2 sidumispotentsiaali hindamisel tuleks arvestada ka kaltsiumsilikaatide ($CaSiO_3$ ja Ca_2SiO_4) ning periklaasiga.

Protsessi pidurdumismehhanismi selgitamiseks uuriti lubja, kui antud süsteemis ühe olulisima tuha komponendi, käitumist erinevates tingimustes. Leiti, et vähepoorsete tolmpõletustuhade puhul pidurdub karboniseerimisprotsess märgatavalt. Kõrge soolsusega ringlusvee toimel $Ca(OH)_2$ difusioon lahusesse aeglustub, mis vähendab omakorda lubja kutsumiskiirust ning tingib reaktsioonide toimumise pooride suudmeis. Sadestuvad reaktsiooniproduktid nagu $CaCO_3$ ja $CaSO_4$ võivad kas osaliselt või täielikult peatada vaba lubja edasise lahustumise. Keevkihttuhade poorne struktuur soodustab nii lubja kiiret ja täielikku kustumist kui ka Ca^{2+}-ioonide difusiooni lahusesse, tagades seega peaaegu täieliku karboniseerimise.

Koostati kontseptsioon süsihappegaasi emissiooni vähendamiseks põlevkivienergeetikas samas tekkivate tuhkade baasil kõigi CO_2 mineraliseerimisvõimaluste süsteemse arvestamisega. Töötati välja põhiparameetrid CO_2 märgsidumiseks suitsugaasidest nii otsese (tuha vesisuspensioonid) kui ka kaudse (tuha transpordiveed) karboniseerimise teel. Tulemused on kasutatavad alusmaterjalina tööstusliku katseaparatuuri kavandamisel.

Töötati välja uudne meetod leeliselise Ca^{2+}-ioone sisaldava heitvee intensiivseks neutraliseerimiseks suitsugaasides sisalduva süsinikdioksiidiga. Näidati, et

leeliseline tuha transpordivesi on perspektiivne tooraine romboeedrililise struktuuri ning homogeense tükisuurusega (~5µm) sadestatud kaltsiumkarbonaadi (PCC) tootmiseks. CO_2 emissiooni Eesti põlevkivienergeetikast on võimalik vähendada kasutades samas tekkivaid tuhkasid CO_2 sorbentidena: kokku on võimalik siduda (karboniseerimisprotsessis ja ladustamise käigus) 192–209 kg CO_2 tonni tuha kohta või 10–11% ja 60–65% vastavalt põlevkivi põletamisel eralduva CO_2 koguemissioonist ja põlevkivi mineraalosast pärinevast CO_2 emissioonist.

APPENDIX A

Paper I

Kuusik R., Türn L., Trikkel A., *Uibu M*.

Carbon dioxide binding in the heterogeneous systems formed at combustion of oil shale. 2. Interactions of system components – thermodynamic analysis.

Paper II

Kuusik, R., *Uibu, M.,* Kirsimäe, K.

Characterization of oil shale ashes formed at industrial-scale CFBC boilers.

Paper III

Uibu, M., Uus, M., Kuusik, R.

CO$_2$ mineral sequestration by oil shale wastes from Estonian power production.

Reprinted with permission from:

Journal of Environmental Management. **2008**

Paper IV

Uibu, M., Kuusik, R.

Mineral trapping of CO_2 via oil shale ash aqueous carbonation: rate controlling mechanism and development of the continuous flow reactor system. (In press, manuscript accepted)

Paper V

Uibu, M., Velts, O., Trikkel, A., Kuusik, R.

Reduction of CO_2 emissions by carbonation of alkaline wastewater.

ELULOOKIRJELDUS

1. Isikuandmed

    Ees- ja perekonnanimi   Mai Uibu
    Sünniaeg ja -koht   20.08.1979 Tallinn
    Kodakondsus   Eesti

2. Kontaktandmed

    Aadress   Keskuse 22-53, Tallinn, Eesti
    Telefon   5214319
    E-posti aadress   maiuibu@staff.ttu.ee

3. Hariduskäik

Õppeasutus (nimetus lõpetamise ajal)	Lõpetamise aeg	Haridus (eriala/kraad)
Tallinna Tehnikaülikool	2004	Tehnikateaduste magistrikraad
Tallinna Tehnikaülikool	2001	Tehnikateaduste bakalaureusekraad
Tallinna 49. Keskkool	1997	Keskharidus

4. Keelteoskus (alg-, kesk- või kõrgtase)

Keel	Tase
Eesti keel	Kõrgtase
Inglise keel	Kõrgtase
Vene keel	Algtase

5. Täiendusõpe

Õppimise aeg	Täiendusõppe läbiviija nimetus
29.09–01.10.2003	CO_2 course in Trondheim, NTNU Trondheim
17.11–19.11.2003	Greenhouse Gas Emissions Control and CO_2 Long Term Storage, Helsingi Tehnikaülikool
27.09–30.09.2004	Ph.D. Course CO_2 Capture and Storage, Chalmersi Tehnikaülikool
5.09–7.09.2005	Nordic post-graduate course on CO_2 capture and storage, Helsingi Tehnikaülikool
1.04– 4.04.2006	Talvekool "Nüüdismaterjalid ja protsessid", UTTP doktorikool
2.05–26. 05.2006	Helsingi Tehnikaülikool
22.02–23.02.2007	Talvekool, UTTP doktorikool
15.08–17.08.2007	Suvekool, UTTP doktorikool

6. Teenistuskäik

Töötamise aeg	Tööandja nimetus	Ametikoht
2005–2008	Tallinna Tehnikaülikool, Uute tootmistehnoloogiate ja -protsesside doktorikool	Erakorraline teadur
2004–…	Tallinna Tehnikaülikool, Anorg. materjalide teaduslaboratoorium	Teadur
2002–2004	Tallinna Tehnikaülikool, Keemiatehnika instituut	Insener
1997	Tallinna Maksuamet	Sekretär

7. Kaitstud lõputööd

Magistritöö: CO_2 mineraliseerimine põlevkivienergeetikas. Tallinna Tehnikaülikool, 2004. Juhendaja R: Kuusik
Bakalaureusetöö: Põlevkivituha vesisuspensiooni karboniseerimine. Tallinna Tehnikaülikool, 2001. Juhendaja: R. Kuusik

8. Teadustöö põhisuunad

Heterogeensed reaktsioonid põlevkivituha baasil tekkivates süsteemides.

Projektid:
237L Happeliste gaaside emissiooni vähendamine (2002)
323L Põlevkivituha karboniseerimine (2003–2008)
Lep7017 Põlevkivituhk kaltsiumkarbonaadi toormena (2007–2008)
V215 Nordic CO_2 Sequestration (2003–2007)
SF0142518s03 Anorgaaniliste mitmekomponentsete süsteemide keemia ja rakendused (2003–2007)
ETF6195 Ringlevas keevkihis tekkivad põlevkivituhad happeliste gaaside sorbendina (2005–2007)
Lep7096A Süsihappegaasi heitkoguste mineraalse sidumise ja geoloogilise ladustamise võimaluste hindamine tehnoloogiliselt, geoloogiliselt ja toksikoloogiliselt (2007)
SF0140082s08 Karbonaat- ja fosfaatpõhiste anorgaaniliste süsteemide keemia ja rakendused (2008–2013)
ETF7379 Süsinikdioksiidi mineraliseerimisprotsesside modelleerimine (2008–2011)

CURRICULUM VITAE

1. Personal data

Name	Mai Uibu
Date and place of birth	20.08.1979, Tallinn, Estonia

2. Contact information

Address	Keskuse 22-53, Tallinn, Estonia
Phone	5214319
E-mail	maiuibu@staff.ttu.ee

3. Education

Educational institution	Graduation year	Education (field of study/degree)
Tallinn University of Technology	2004	M. Sc. in Engineering
Tallinn University of Technology	2001	B. Sc. in Engineering
Tallinn 49. Secondary School	1997	High school education

4. Language competence/skills (fluent; average, basic skills)

Language	Level
Estonian	Fluent
English	Fluent
Russian	Basic skills

5. Special Courses

Period	Educational or other organisation
29.09–01.10.2003	CO_2 course in Trondheim, NTNU Trondheim
17.11–19.11.2003	Greenhouse Gas Emissions Control and CO_2 Long-Term Storage, Helsinki University of Technology
27.09–30.09.2004	Ph.D. Course CO_2 Capture and Storage, Chalmers University of Technology
5.09–7.09.2005	Nordic post-graduate course on CO_2 capture and storage, Helsinki University of Technology
1.04-4.04. 2006	Winter school, UTTP Doctoral School
2.05–26.05.2006	Helsinki University of Technology
22.02–23.02.2007	Winter school, UTTP Doctoral School
15.08–17.08.2007	Summer school, UTTP Doctoral School

6. Professional Employment

Period	Organisation	Position
2005–2008	Tallinn University of Technology, UTTP Doctoral School	Extraordinary Researcher
2004–…	Tallinn University of Technology, Laboratory of Inorganic Materials	Researcher
2002–2004	Tallinn University of Technology, department of Chemical Engineering	Engineer
1997	Tallinn Tax Office for Legal Entities	Secretary

7. Defended theses

M. Sc. thesis: Mineralization of CO_2 in oil shale based energetics Tallinn University of Technology, 2004. Supervisor: R. Kuusik
B. Sc. thesis: Carbon dioxide binding in the aqueous suspensions of oil shale ash. Tallinn University of Technology, 2001. Supervisor: R. Kuusik.

8. Main areas of scientific work/Current research topics

Heterogeneous reactions in oil shale ash based systems.

Projects:
323L Carbonation of oil shale ash (2003–2008)
Lep7017 PCC from oil shale ash (2007–2008)
V215 Nordic CO_2 Sequestration (2003–2007)
SF0142518s03 Chemistry and applications of inorganic multicomponent systems (2003–2007)
ETF6195 Oil shale ashes formed in circulating fluidized bed as sorbents for acidic gases (2005–2007)
Lep7096A Technological, geological and toxicological assessment of mineralization of CO_2 emissions. (2007)
SF0140082s08 Chemistry and applications of carbonate-phosphate-based inorganic systems (2008–2013)
ETF7379 Modelling of carbon dioxide mineralization processes (2008–2011)